Microscopie de force dynamique: éléments (Deuxième partie)

Laurent Nony

Microscopie à Force Atomique (AFM) en mode dynamique: éléments Deuxième partie

Laurent Nony
laurent.nony @im2np.fr

Séminaire interne, Juin 2006

Université Paul Cézanne Aix-Marseille III
IM2NP - UMR CNRS 6242
Marseille

Introduction au non-contact AFM (ou FM-AFM)

- nc-AFM *vs.* “Tapping” ou modulation de fréquence *vs.* modulation d’amplitude
- Réelle méthode de non-contact
- Sensibilité verticale trés supérieure au “Tapping”
- Méthode de découplage efficace des forces conservatives et dissipatives (pourvu que la phase soit bien maintenue)
- Affranchissement de la constante de temps liée au facteur de qualité
- Technique essentiellement UHV (requiert Q élevé)
- Contribution potentielle de l’électronique aux signaux de mesure !

Le non-contact AFM

Phase fixée (=-90°) et
amplitude d'oscillation fixée
(modulation de fréquence)

↓

Mesures : décalage de la fréquence de résonance et amplitude d'excitation requise pour conserver l'amplitude d'oscillation constante en fonction de la distance pointe-surface

Asservissement : décalage donné de la fréquence de résonance

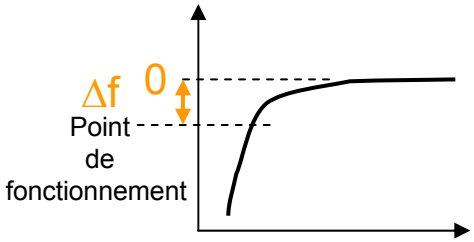

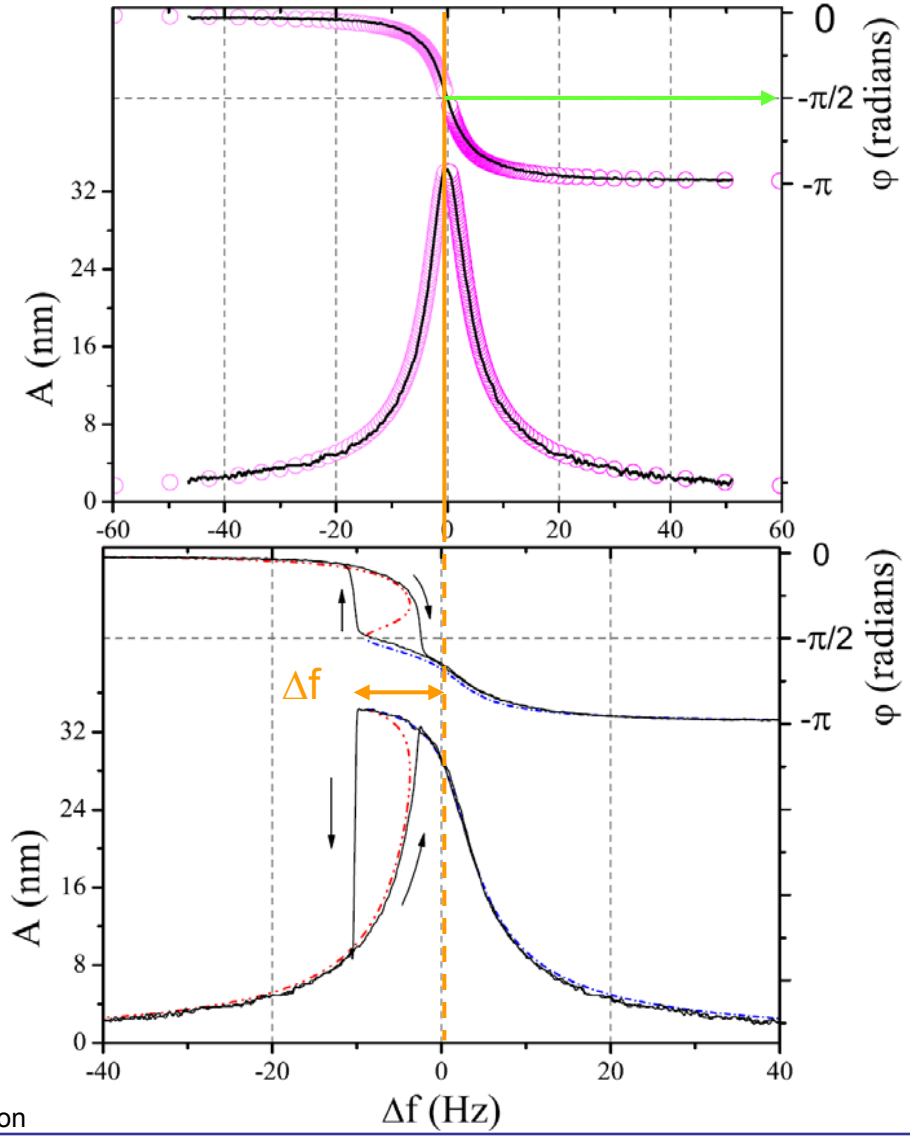

Mesure d'effets dissipatifs en nc-AFM

- Energie dissipée par un oscillateur harmonique

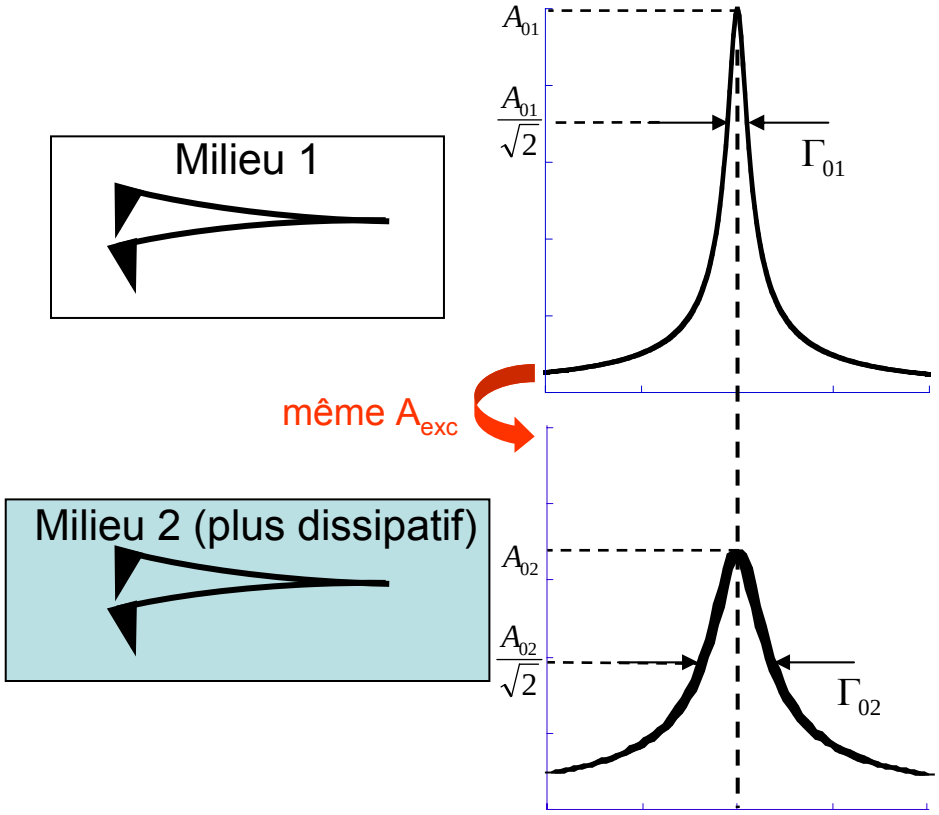

$$Q_{01} = \frac{\omega_0}{\Gamma_{01}}$$

$$Q_{02} = \frac{\omega_0}{\Gamma_{02}}, \Gamma_{02} >> \Gamma_{01} \Rightarrow Q_{02} << Q_{01}$$

$$A_{0i} = Q_{0i} A_{exc} \Rightarrow A_{02} << A_{01}$$

$$Q = 2\pi \frac{\langle E_{stored} \rangle_T}{\langle E_{diss} \rangle_T} \Leftrightarrow \langle E_{diss} \rangle_T = 2\pi \frac{\langle E_{stored} \rangle_T}{Q} \Rightarrow \langle E_{diss} \rangle_T = \pi \frac{kA_0^2}{Q} = \pi k A_0 A_{exc} = \pi \frac{kA_0^2 \Gamma_0}{\omega_0}$$

$$A_{exc} \propto \langle E_{diss} \rangle_T \propto \Gamma_0$$

Mesure d'effets dissipatifs en nc-AFM

• Le cas du nc-AFM :

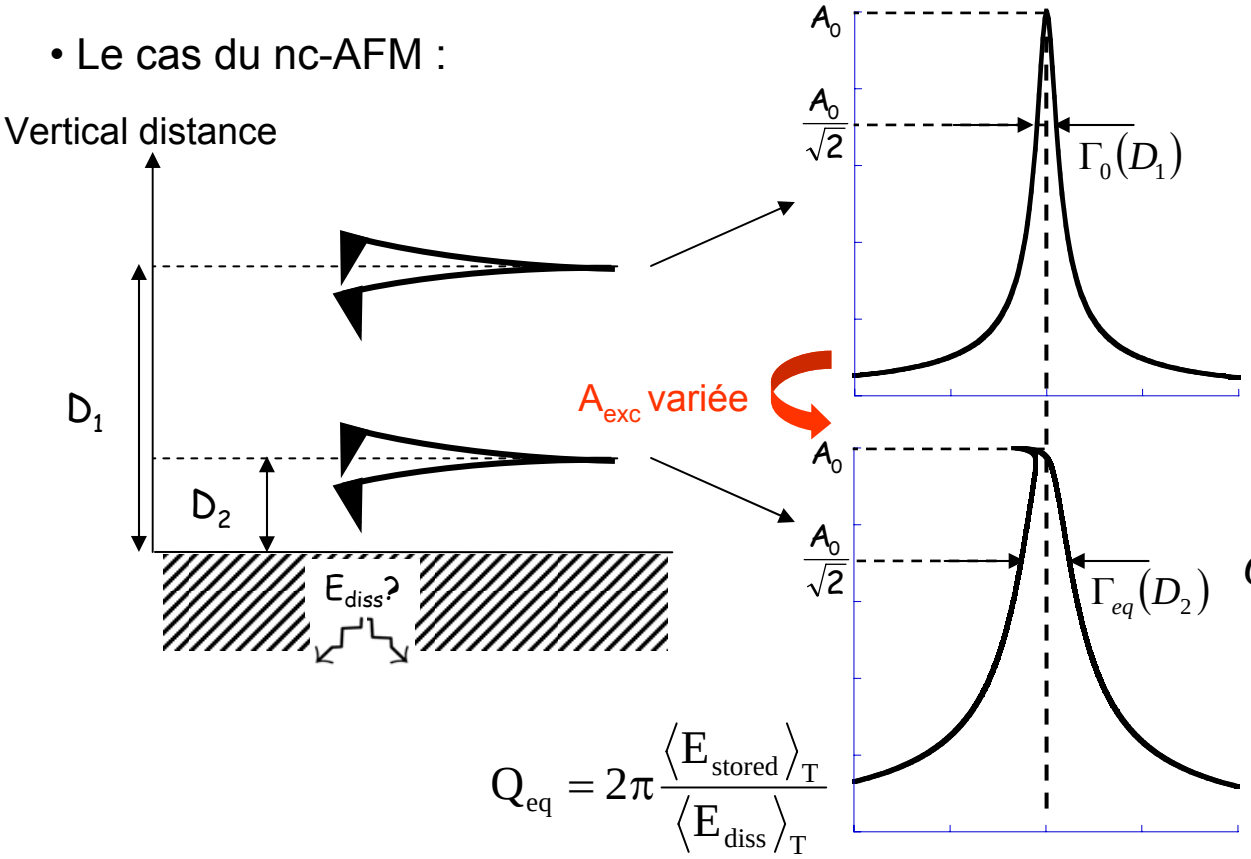

$$Q_0(D_1) = \frac{\omega_0}{\Gamma_0(D_1)}$$

$$Q_{eq}(D_2) = \frac{\omega_0^{nl}}{\Gamma_{eq}(D_2)} \approx \frac{\omega_0}{\Gamma_0 + \Gamma_{int}},$$

avec $\Gamma_{eq} > \Gamma_0$, donc $Q_{eq} < Q_0$

$$Q_{eq} = 2\pi \frac{\langle E_{stored} \rangle_T}{\langle E_{diss} \rangle_T}$$

En nc-AFM, A_0 étant constante → mesure de la dissipation en non-contact

$$\langle E_{diss} \rangle_T = \pi\, k A_0 A_{exc} = \pi\, \Gamma_{eq}(D) \frac{k_0 A_0^2}{\omega_0} \Longrightarrow$$

Les variations de A_{exc} pour conserver A_0 constante forment une image de "dissipation (ou damping)"

Ordres de grandeur (@RT) :
k = 30 N/m
A_0 = 10 nm
$A_{exc}=A_0/Q$ = 10/30000 ~ 0.3 pm
$\langle E_{diss} \rangle_T = 2$ eV/cycle

Illustrations expérimentales

• Signal de dissipation (contrôle sur le Δf) :

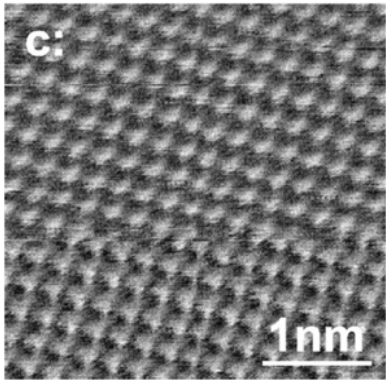

Cu(100)

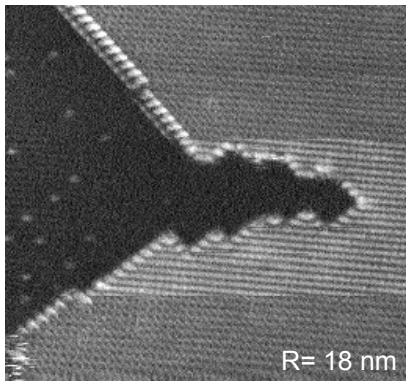

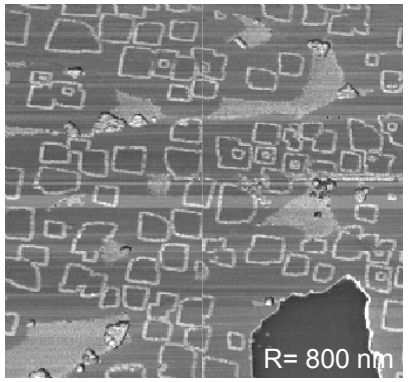

NaCl / Cu(111)

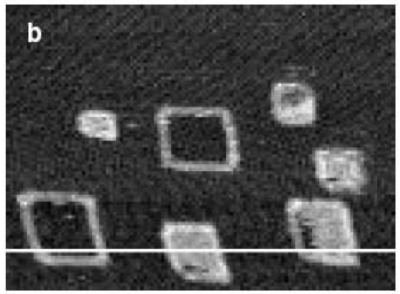

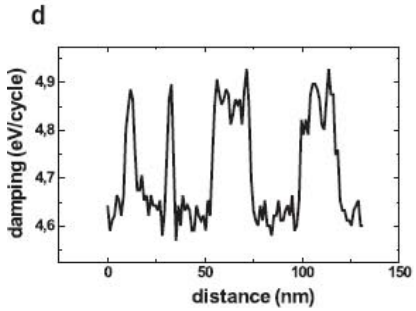

KBr+e⁻+PTCDA

• Contrôle sur courant tunnel :

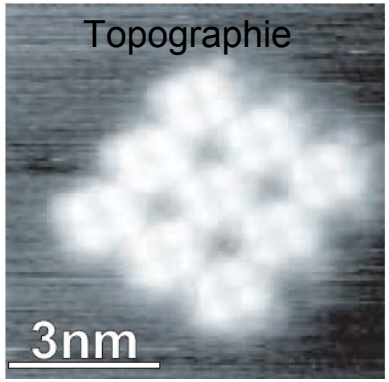

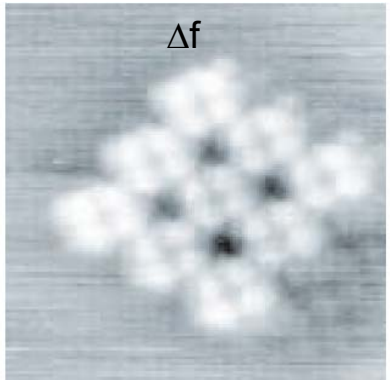

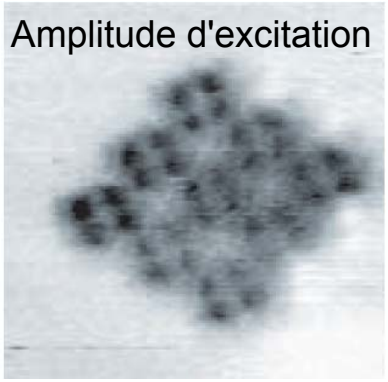

Porphyrines sur Cu(100)

Problématique actuelle en nc-AFM

• Dissipation à l'échelle atomique : **canaux de dissipation** ?

Approche viscoélastique

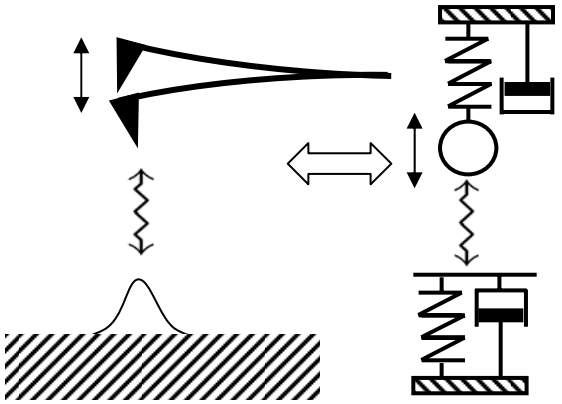

Terme de couplage :
force d'interaction

Approche continue : OK sur des polymères (300 kHz), mais à l'échelle atomique?

Instabilités atomiques (hystérésis d'adhésion)

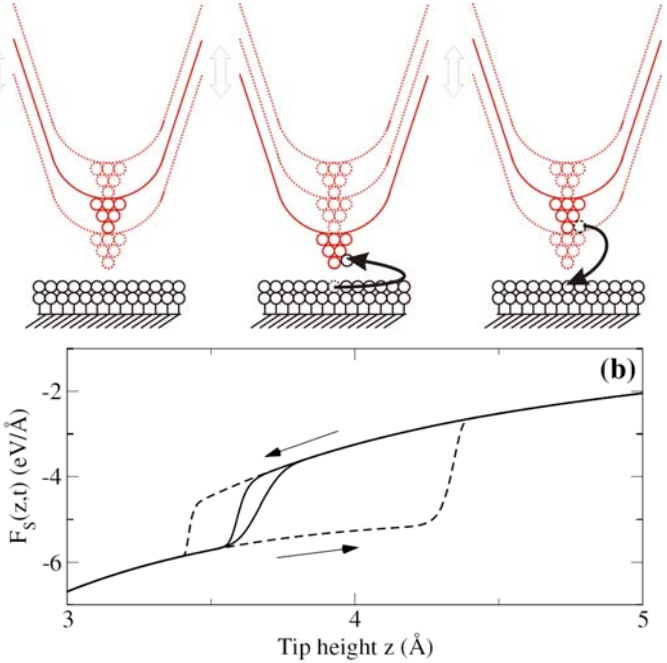

Ordres de grandeurs compatibles avec les résultats expérimentaux.
Mais s'il n'existe pas de "mode mou" en surface (défaut, marche)?

Rôle de l'instrumentation
Dissipation apparente

1

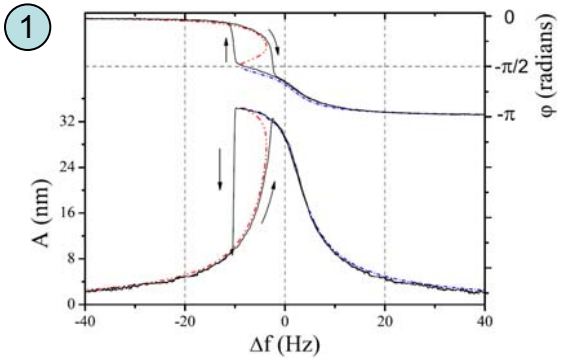

2 Vitesse d'asservissement des contrôleurs en relation avec le balayage

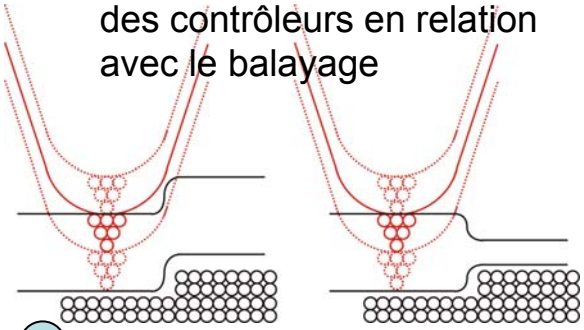

3 Altération du fonctionnement des contrôleurs à cause de la non-linéarité

Dans tous les cas : dissipation induite par le régime attractif

Problématqieu actuelle en nc-AFM

PRL 97, 016103 (2006) PHYSICAL REVIEW LETTERS week ending 7 JULY 2006

Identification of Nanoscale Dissipation Processes by Dynamic Atomic Force Microscopy

R. Garcia,[1,*] C. J. Gómez,[1] N. F. Martinez,[1] S. Patil,[1] C. Dietz,[2] and R. Magerle[2]

[1]*Instituto de Microelectrónica de Madrid, CSIC, Isaac Newton 8, 28760 Tres Cantos, Madrid, Spain*
[2]*Chemische Physik, Technische Universität Chemnitz, D-09107 Chemnitz, Germany*

(Received 11 April 2006; published 7 July 2006)

Identification of energy-dissipation processes at the nanoscale is demonstrated by using amplitude-modulation atomic force microscopy. The variation of the energy dissipated on a surface by a vibrating tip as a function of its oscillation amplitude has a shape that singles out the dissipative process occurring at the surface. The method is illustrated by calculating the energy-dissipation curves for surface energy hysteresis, long-range interfacial interactions and viscoelasticity. The method remains valid with independency of the amount of dissipated energy per cycle, from 0.1 to 50 eV. The agreement obtained between theory and experiments performed on silicon and polystyrene validates the method.

A nc-AFM simulator with PLL-controlled frequency detection and excitation : addressing the problem of apparent dissipation

L. Nony, A. Baratoff, D. Schär, A. Wetzel, O. Pfeiffer,
R. Bennewitz* and E. Meyer

June 2004

NCCR on Nanoscale Science,
Institute of Physics, Basel, Switzerland
** Mc Gill University, Montreal, Canada*

Motivations

Why a virtual machine?

- Assessing the contribution of the instrumentation to the measurements
  - **apparent dissipation**
  - what component, how…
  - time constants of the system, establishing a hierarchy

Dissipation vs. apparent dissipation

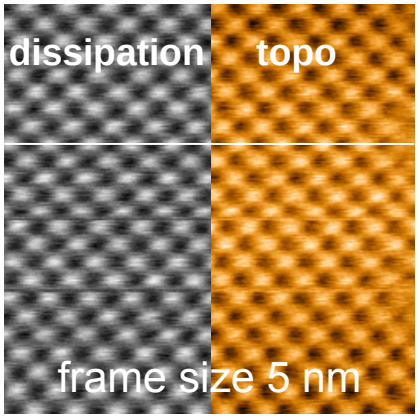

topography and dissipation are neither correlated nor anti-correlated

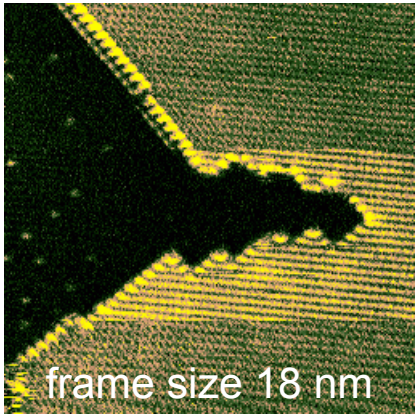

Enhanced dissipation at steps (100 meV/cycle)

VOLUME 89, NUMBER 14 PHYSICAL REVIEW LETTERS 30 SEPTEMBER 2002

Interplay between Nonlinearity, Scan Speed, Damping, and Electronics in Frequency Modulation Atomic-Force Microscopy

Michel Gauthier,[1] Ruben Pérez,[2] Toyoko Arai,[3] Masahiko Tomitori,[3] and Masaru Tsukada[1]
[1]*Department of Physics, Graduate School of Science, University of Tokyo, Hongo 7-3-1, Bunkyo-ku, Tokyo 113-0033, Japan*
[2]*Departamento de Física Teórica de la Materia Condensada, Universidad Autónoma de Madrid, E-28049 Madrid, Spain*
[3]*School of Materials Science, Japan Advanced Institute of Science and Technology, 1-1 Asahidai, Tatsunokuchi, Nomi-gun, Ishikawa 923-1292, Japan*
(Received 23 March 2002; published 16 September 2002)

Numerical simulations of the frequency modulation atomic force microscope, including the whole dynamical regulation by the electronics, show that the cantilever dynamics is conditionally stable and that there is a direct link between the frequency shift and the conservative tip-sample interaction. However, a soft coupling between the electronics and the nonlinearity of the interaction may significantly affect the damping. A resonance between the scan speed and the response time of the system can provide a simple explanation for the spatial shift and contrast inversion between topographical and damping images, and for the extreme sensitivity of the damping to a tip change.

REVIEW OF SCIENTIFIC INSTRUMENTS VOLUME 74, NUMBER 5 MAY 2003

Noncontact atomic force microscopy: Stability criterion and dynamical responses of the shift of frequency and damping signal

G. Couturier,[a] R. Boisgard, L. Nony,[b] and J. P. Aimé
Centre de Physique Moléculaire Optique et Hertzienne, Université Bordeaux I, UMR5798 CNRS, 351 Cours de la Libération, 33405 Talence Cedex, France

(Received 23 July 2002; accepted 13 January 2003)

Motivations

Why a virtual machine?

- Assessing the contribution of the instrumentation to the measurements
  - **apparent dissipation**
  - what component, how…
  - time constants of the system, establishing a hierarchy
- Doing physics
  - tip/surface interaction
  - dissipative processes
  - images calculation

nc-AFM electronics : self-excitation scheme

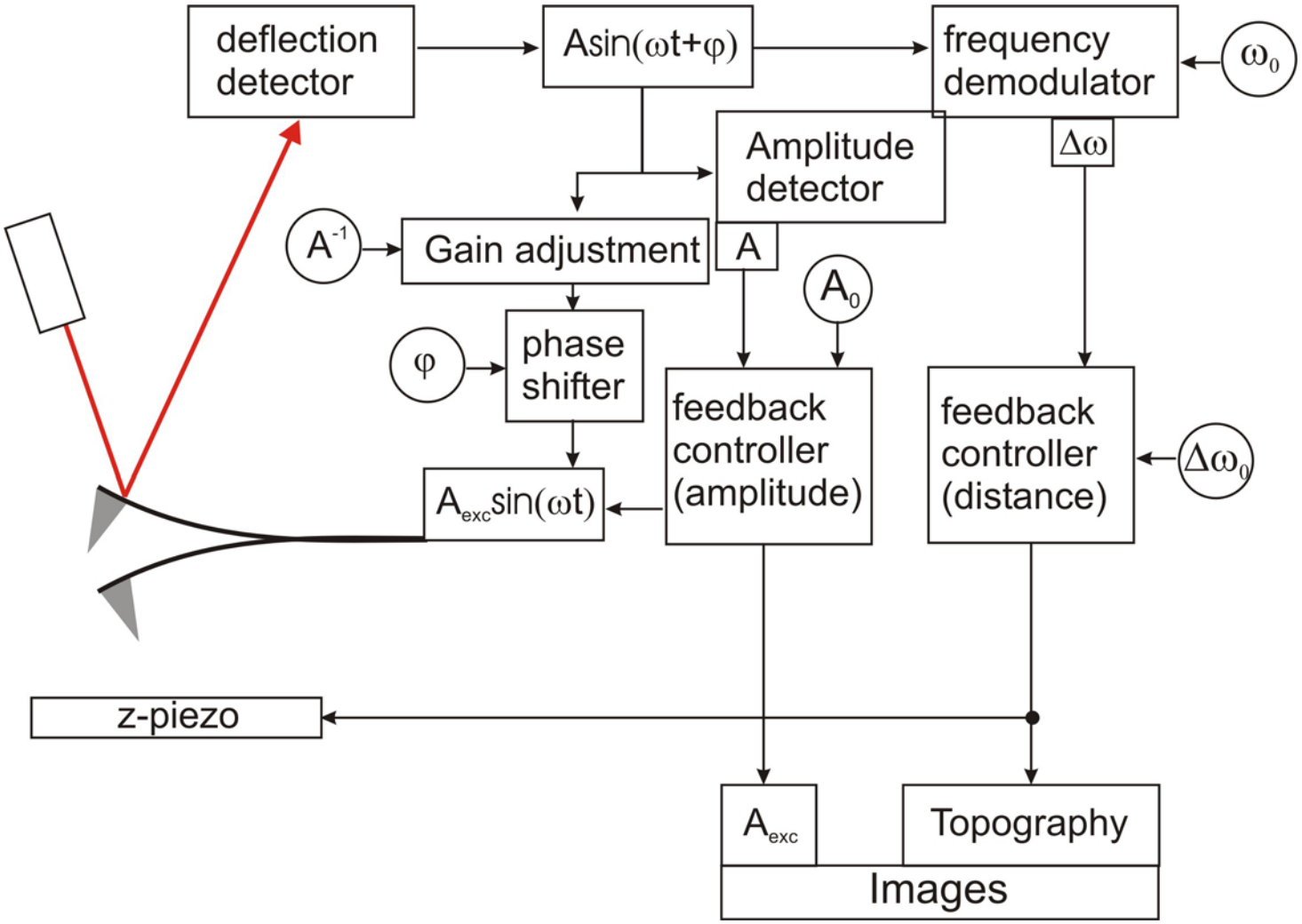

nc-AFM electronics : self-excitation scheme

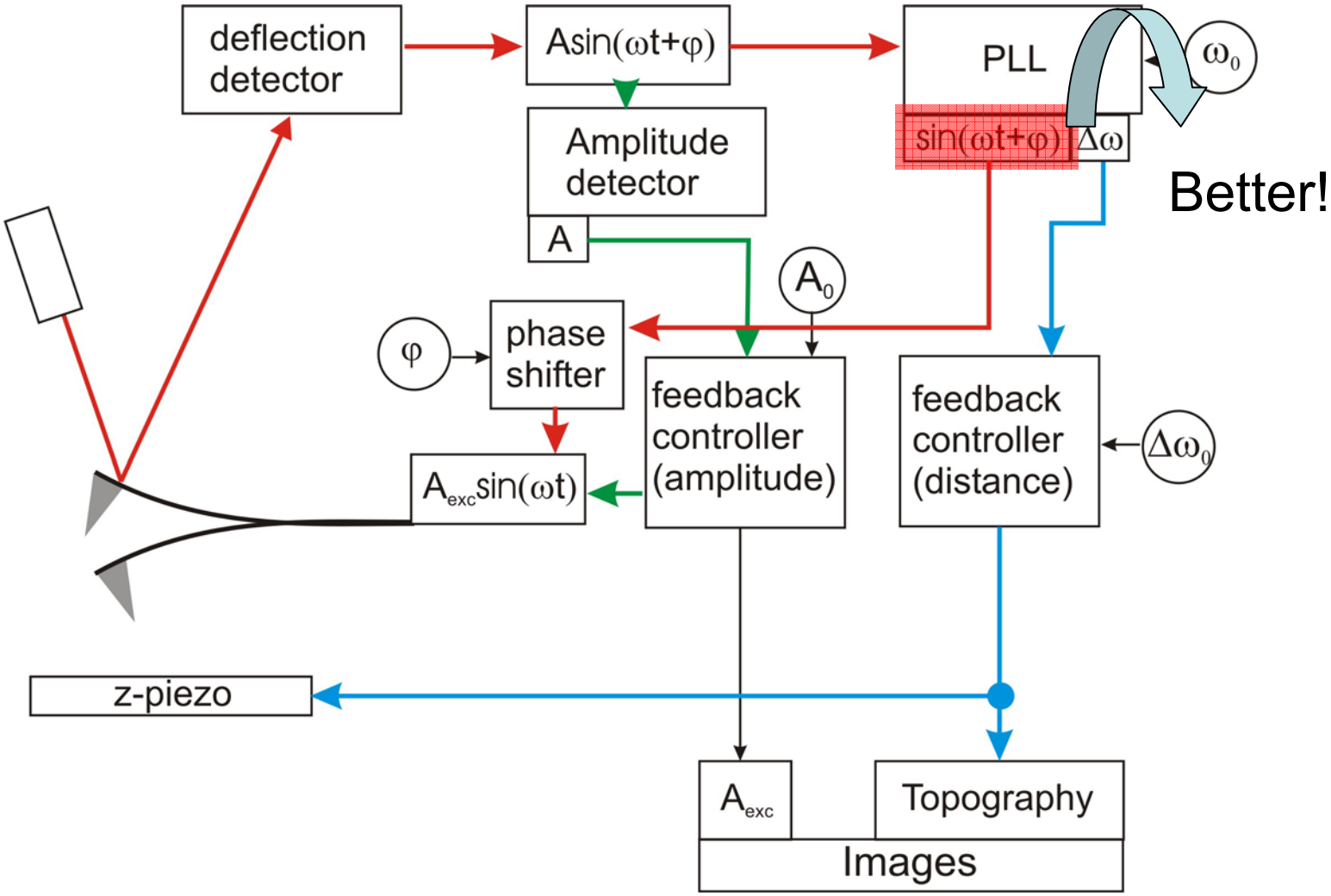

Block diagram of the electronics

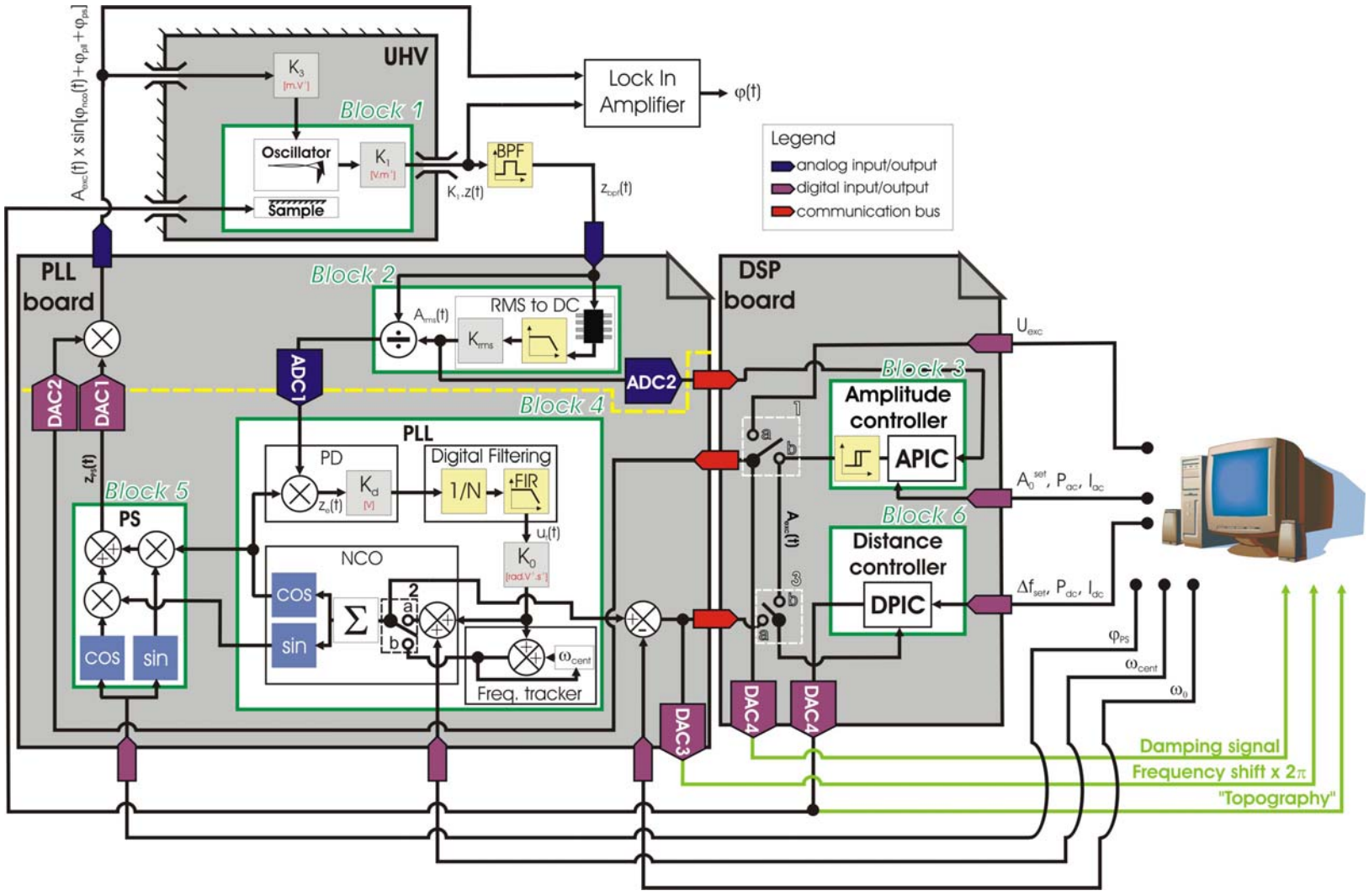

Block diagram of the electronics

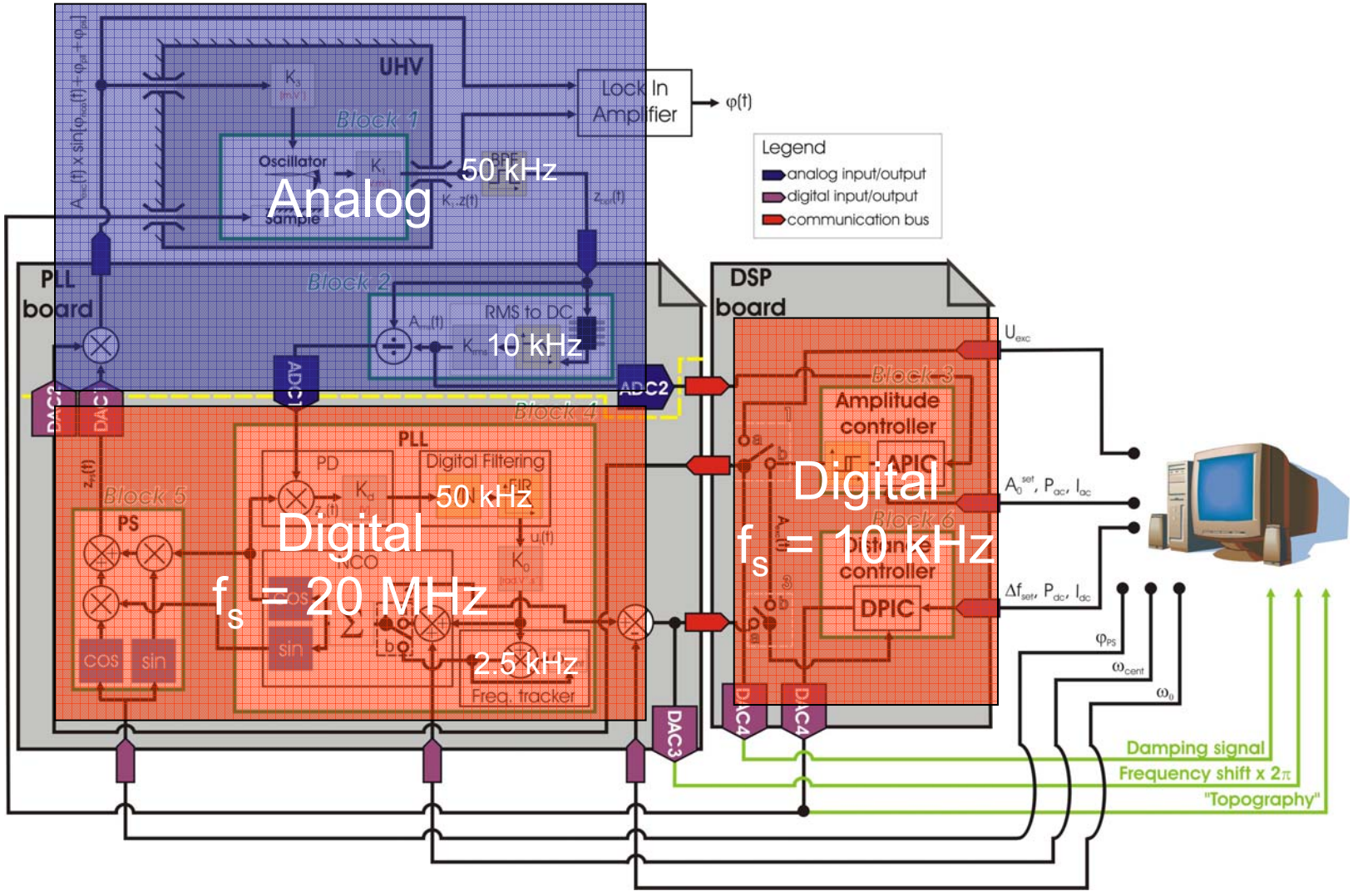

Features

- Description of the real setup (mix of analog/digital devices)
- LabView™ implementation (now C version available)
- GUI with tunable parameters at run time
- The Phase-Locked Loop (PLL) detects the frequency shift and provides the excitation signal to the cantilever

Implementation

- Difficulties :
  - Three (four) feedback loops: PLL, APIC, DPIC
  - Various operating frequencies (many time constants)
  - 3 controllers : 6 gains
  - Non-linear problem with coupled components
- Assumptions :
  - Analog components are solved with a modified Verlet's algorithm (f_s = 400 MHz)
  - DACs and ADCs are "ideal" components
  - PSD and preamp. not described
  - No noise
  - Any physical channel of dissipation is considered

Block diagram of the electronics

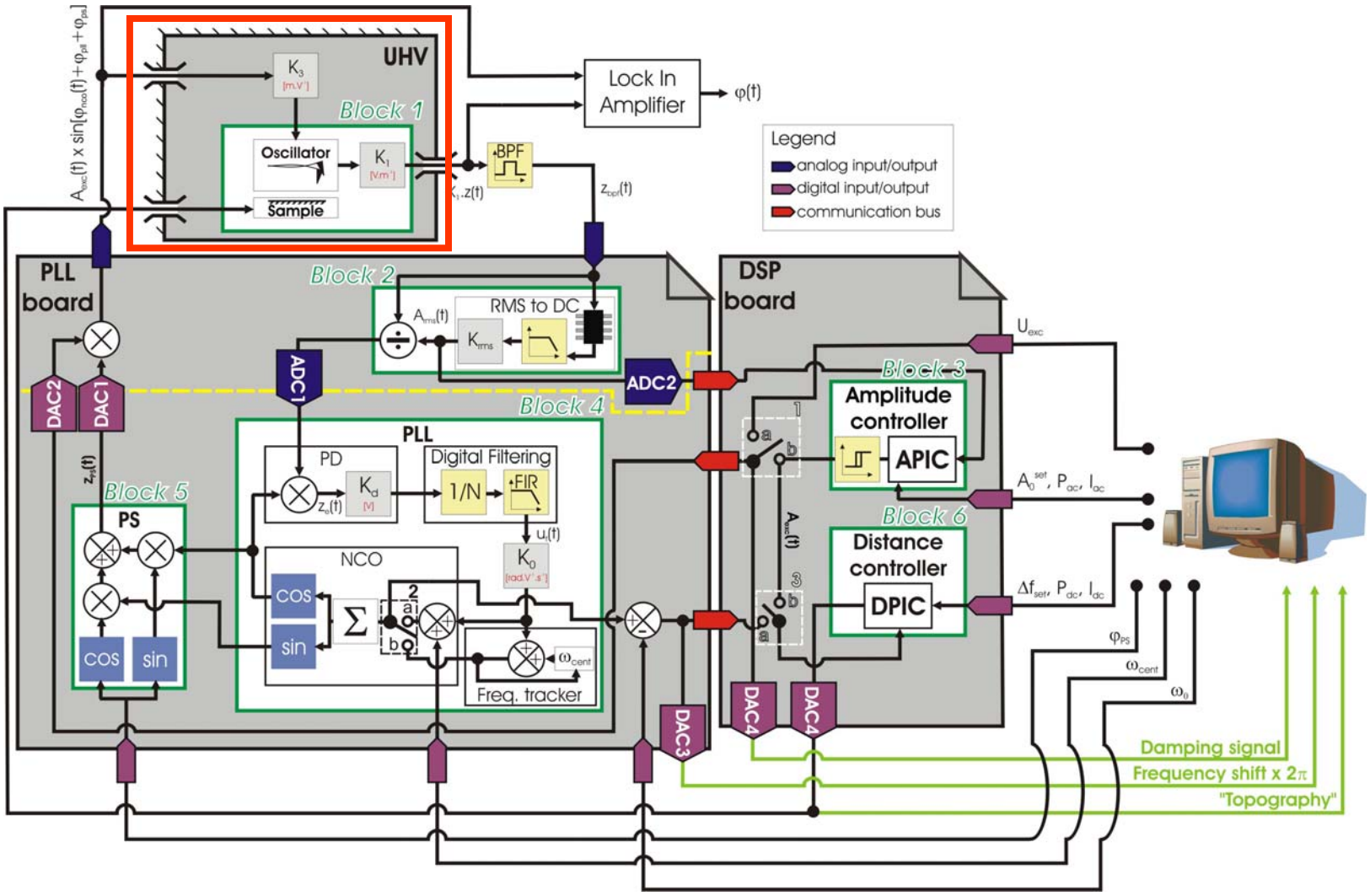

Block 1, the oscillator

From the PLL board (excitation)

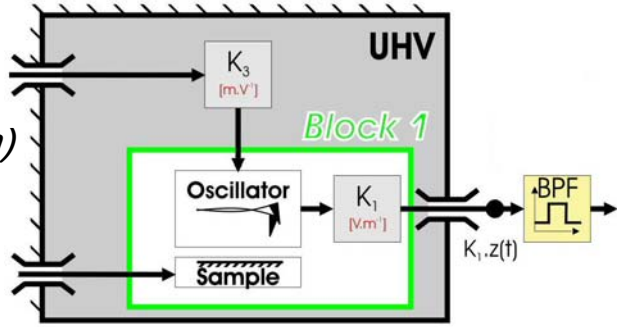

To the PLL board

- Analog device
- $f_s = f_{s_0} = 200$ MHz

Implementation :

$$\ddot{z}(t) + \frac{\omega_0}{Q}\dot{z}(t) + \omega_0^2 z(t) = \omega_0^2 A_{\text{exc}}(t) + \frac{\omega_0^2 F_{\text{int}}(t)}{k_c}$$

$$A_{\text{exc}}(t_i) = K_3 \times D_{amp}(t_i) \times z_{\text{ps}}(t_i)$$

10 kHz 20 MHz

$$\begin{cases} F_{\text{int}}(t) = -\partial_{r(t)} V_{\text{int}}(r(t)) \\ V_{\text{int}}(r) = -\dfrac{HR}{6r} - U_0\left[2e^{-\frac{r-r_c}{\lambda}} - e^{-\frac{2(r-r_c)}{\lambda}}\right] \\ r(t_i) = D(t_i) - z(t_i) \end{cases}$$

BPF output :

$$\ddot{z}_{\text{bpf}}(t) + 2\pi B_W \dot{z}_{\text{bpf}}(t) + \omega_c^2 z_{\text{bpf}}(t) = 2\pi B_W \times K_1 \times \dot{z}(t)$$

50 kHz

Block diagram of the electronics

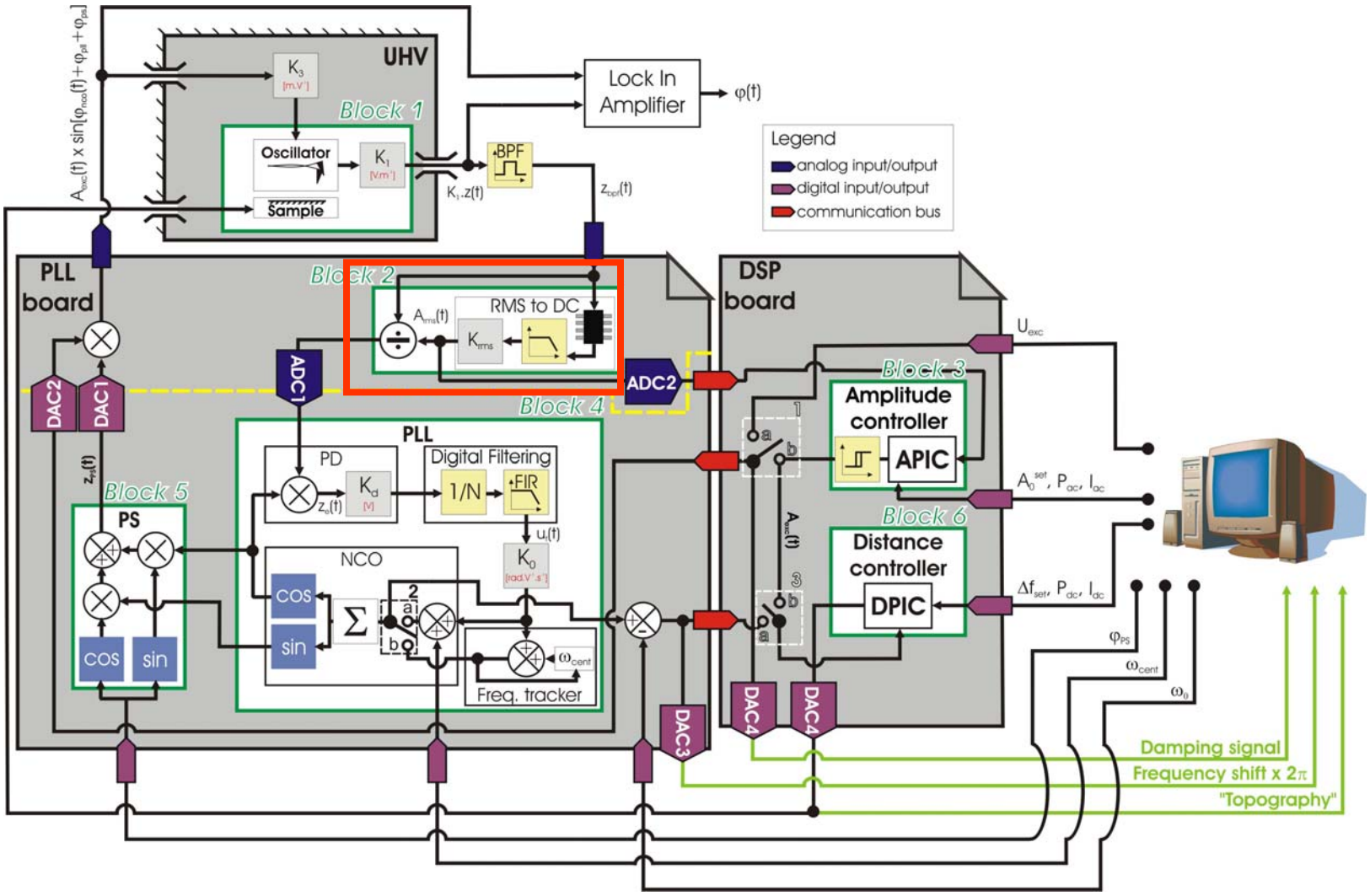

Block 2, the RMS-to-DC converter

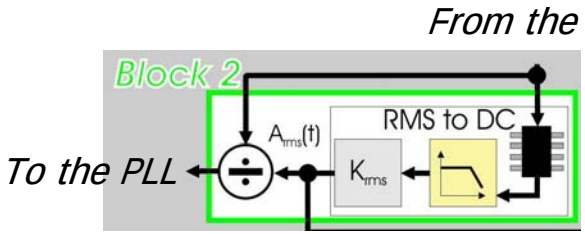

- Analog device (PLL board)
- $f_s = f_{s_0} = 200$ MHz

Implementation :

$$\begin{cases} A_{\mathrm{rms}}(t_i) = K_{\mathrm{rms}} \times \sqrt{V_s(t_i)} \\ \tau_{\mathrm{rms}} \dot{V_s}(t) + V_s(t) = V_e(t) \\ V_e(t_i) = z^2_{\mathrm{bpf}}(t_i) \end{cases}$$

➡ τ_{rms} = 15.9 µs (f_{co}^{lp} = 10 kHz)

The PLL receives : $\dfrac{z_{\mathrm{bpf}}(t_i)}{A_{\mathrm{rms}}(t_i)}$

Block diagram of the electronics

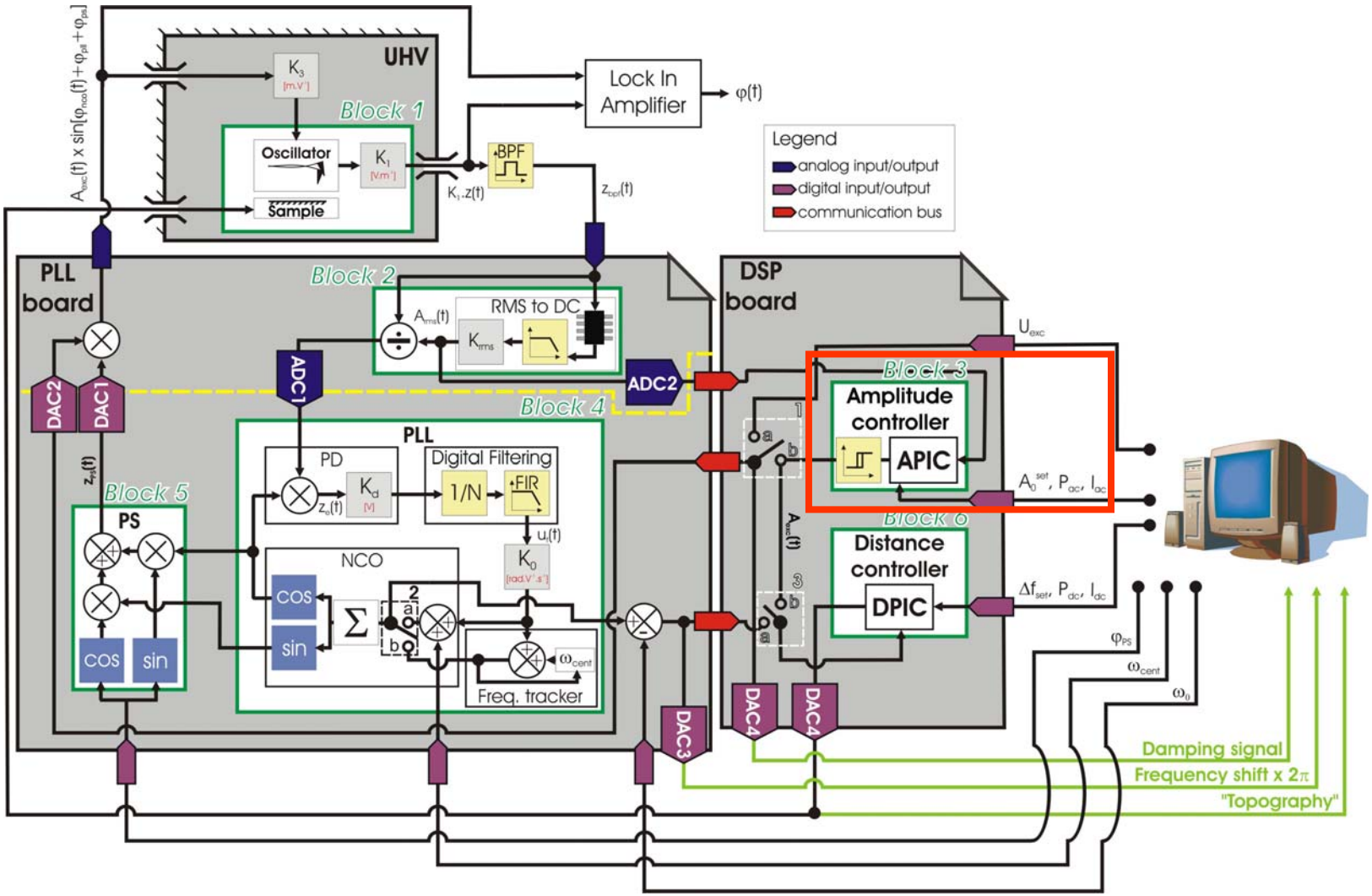

Block 3, the amplitude controller (APIC)

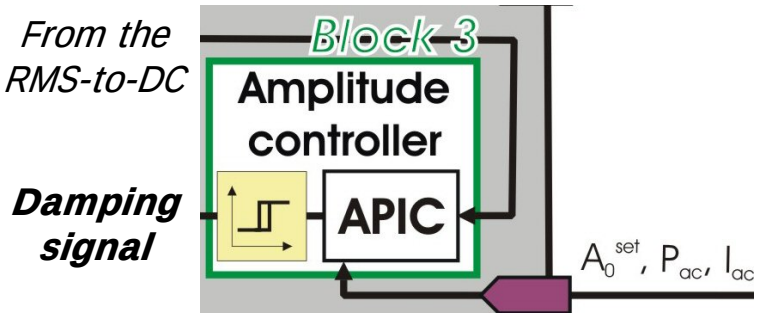

- Digital device (DSP board)
- Provides the output signal @ f_s = 10 kHz

Implementation :

$$D_{amp}(t_i) = P_{\mathrm{ac}}\left[A_0^{\mathrm{set}} - A_{\mathrm{rms}}(t_i)\right] + \sum_{j=0}^{i} I_{\mathrm{ac}}\left[A_0^{\mathrm{set}} - A_{\mathrm{rms}}(t_j)\right]\Delta t_b$$

Saturation : $D_{amp} \in [0\,;10\mathrm{V}]$

Block diagram of the electronics

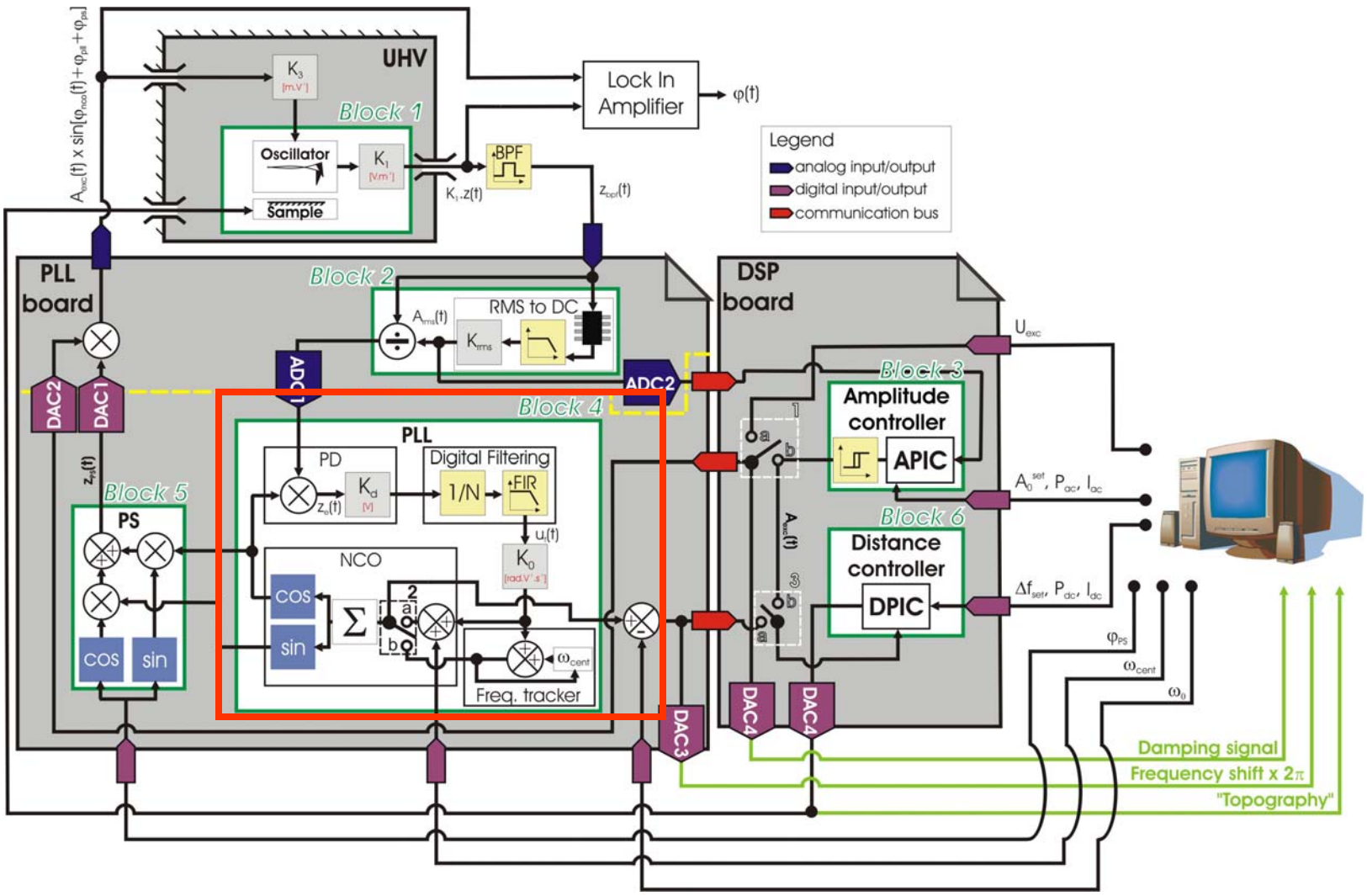

Block 4, the digital PLL

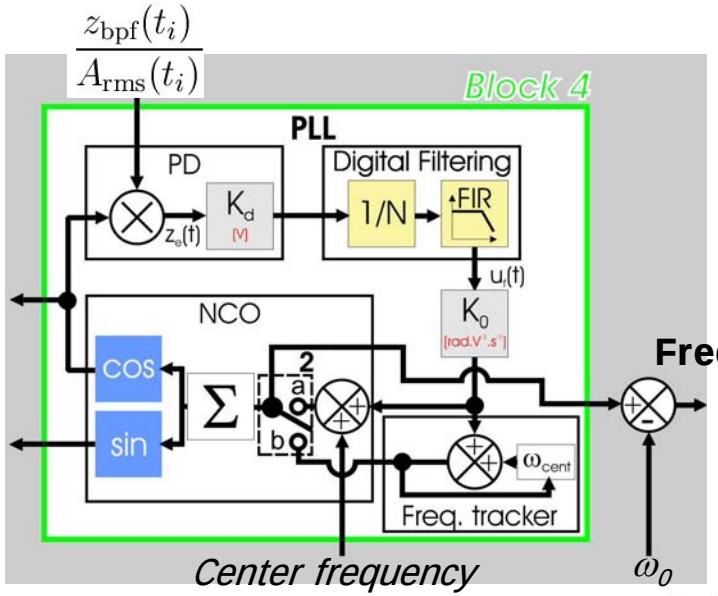

Frequency shift
$2\pi \times \Delta f$

- Digital device (PLL board)
- f_s = 20 MHz

Implementation :

$$z_e(t_i) = \frac{z_{bpf}(t_i)}{A_{rms}(t_i)} \times \cos\left(\varphi_{nco}(t_i)\right)$$

Frequency tracker

Disengaged, ω_{cent} = constant

$$\varphi_{nco}(t_i) = \sum_{j=pll}^{i} \left[\omega_{cent} + K_0 u_f(t_j)\right] \Delta t_c$$

Engaged, ω_{cent} updated (@ 2.5 kHz)

$$\omega_{cent}(t_i) = \omega_{cent}(t_{i-1}) + K_0 \times u_f(t_{i-1})$$

$$\varphi_{nco}(t_i) = \sum_{j=pll}^{i} \omega_{cent}(t_j) \times \Delta t_c$$

Block diagram of the electronics

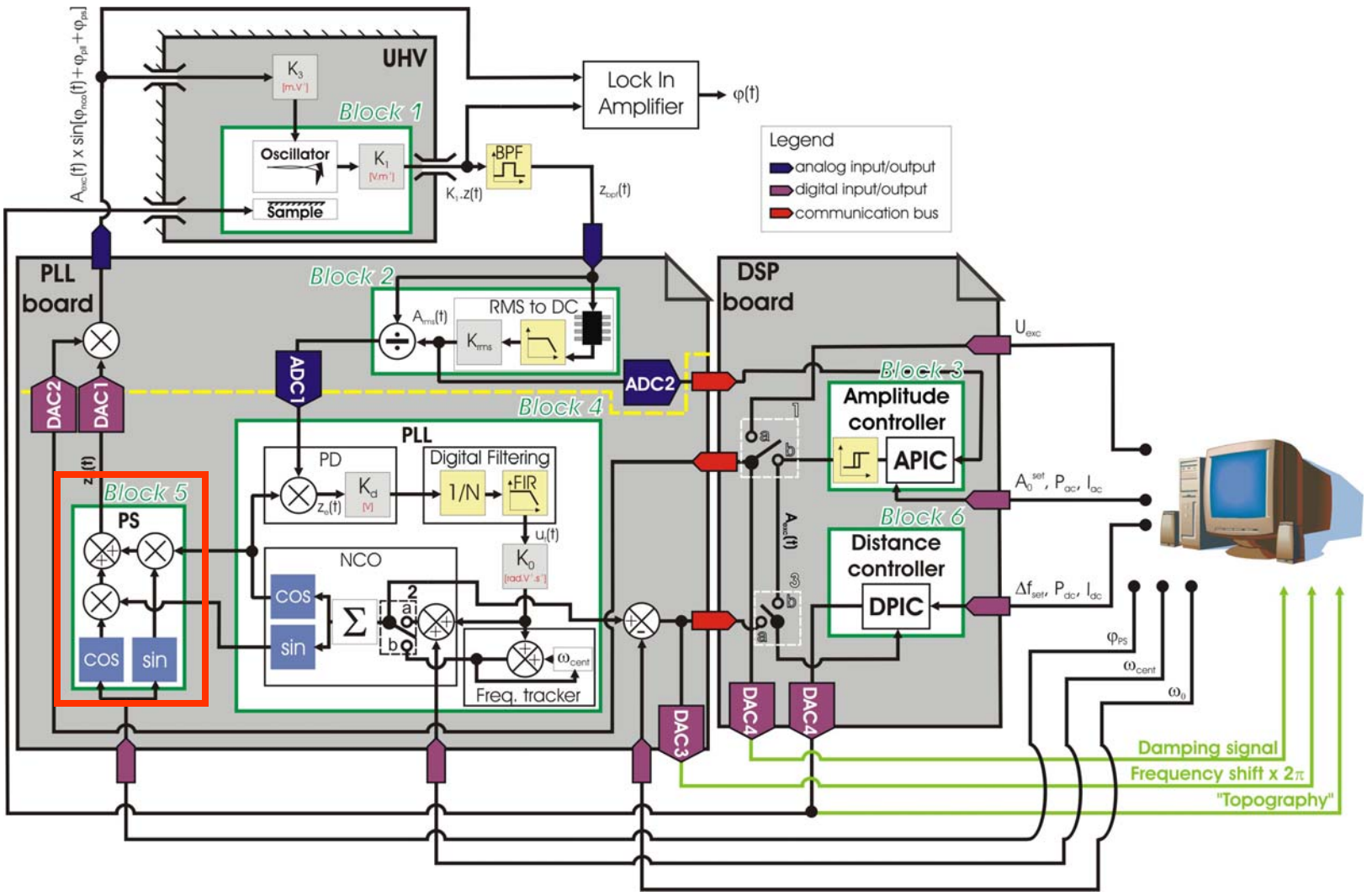

Block 5, the phase shifter

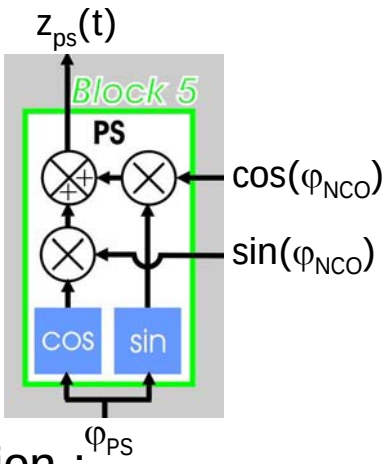

- Digital device (PLL board)
- fs = 20 MHz

Implementation :

$$z_{\mathrm{ps}}(t_i) = \sin\left(\varphi_{\mathrm{nco}}(t_i)\right) \times \cos\left(\varphi_{\mathrm{ps}}\right) + \cos\left(\varphi_{\mathrm{nco}}(t_i)\right) \times \sin\left(\varphi_{\mathrm{ps}}\right)$$
$$= \sin\left(\varphi_{\mathrm{nco}}(t_i) + \varphi_{\mathrm{ps}}\right)$$

Block diagram of the electronics

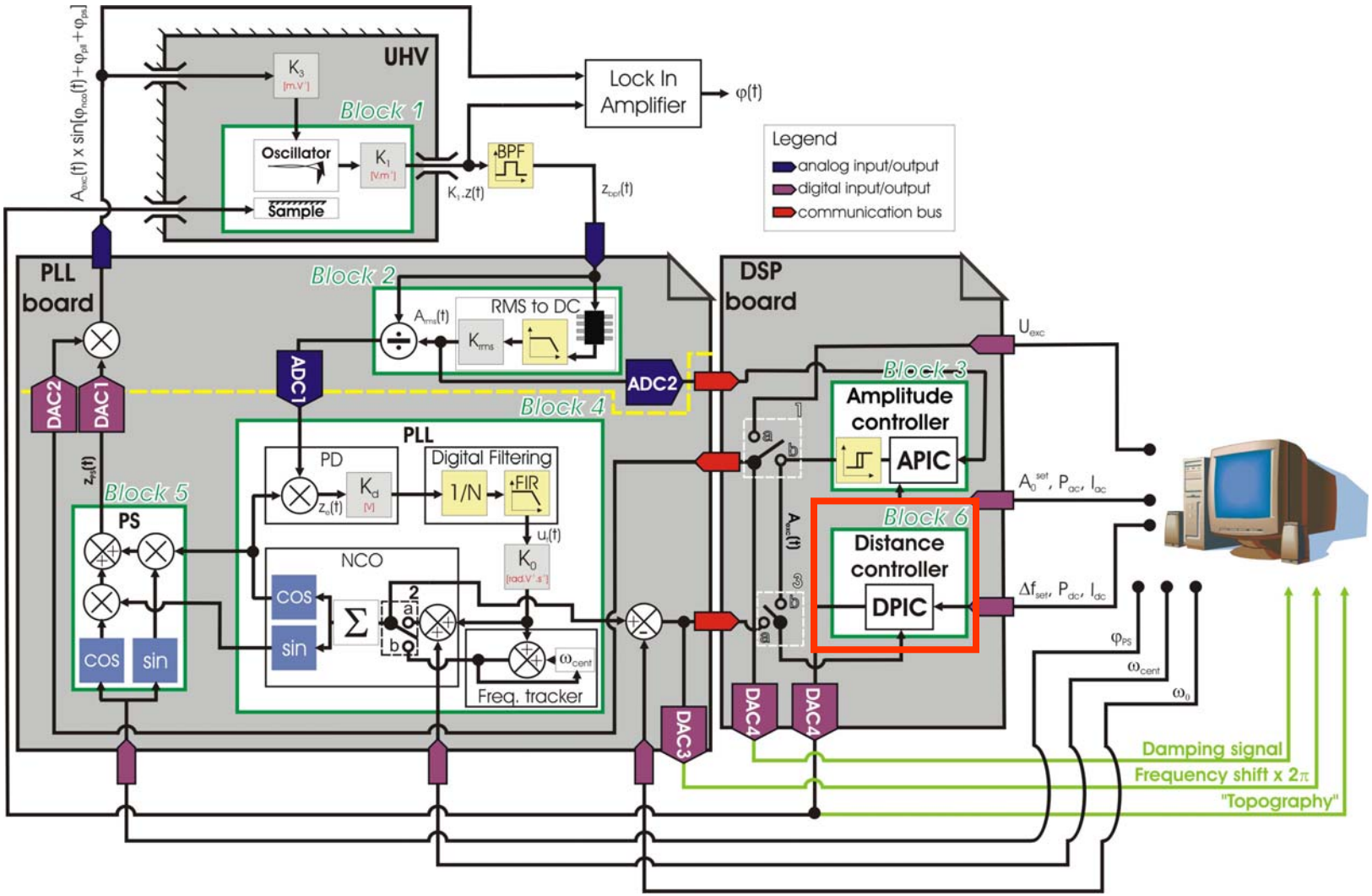

Block 6, the distance controller (DPIC)

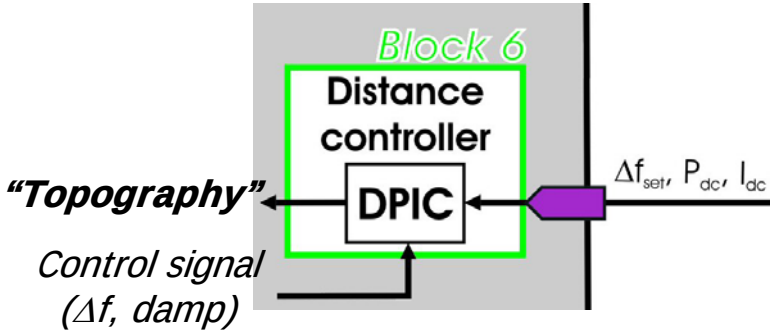

- Digital device (DSP board)
- Provides the output signal @ f_s = 10 kHz

Implementation :

$$D(t_i) = P_{\mathrm{dc}}\left[\Delta f^{\mathrm{set}} - \Delta f(t_i)\right] + \sum_{j=0}^{i} I_{\mathrm{dc}}\left[\Delta f^{\mathrm{set}} - \Delta f(t_j)\right]\Delta t_b$$

Validation of the virtual setup (1)

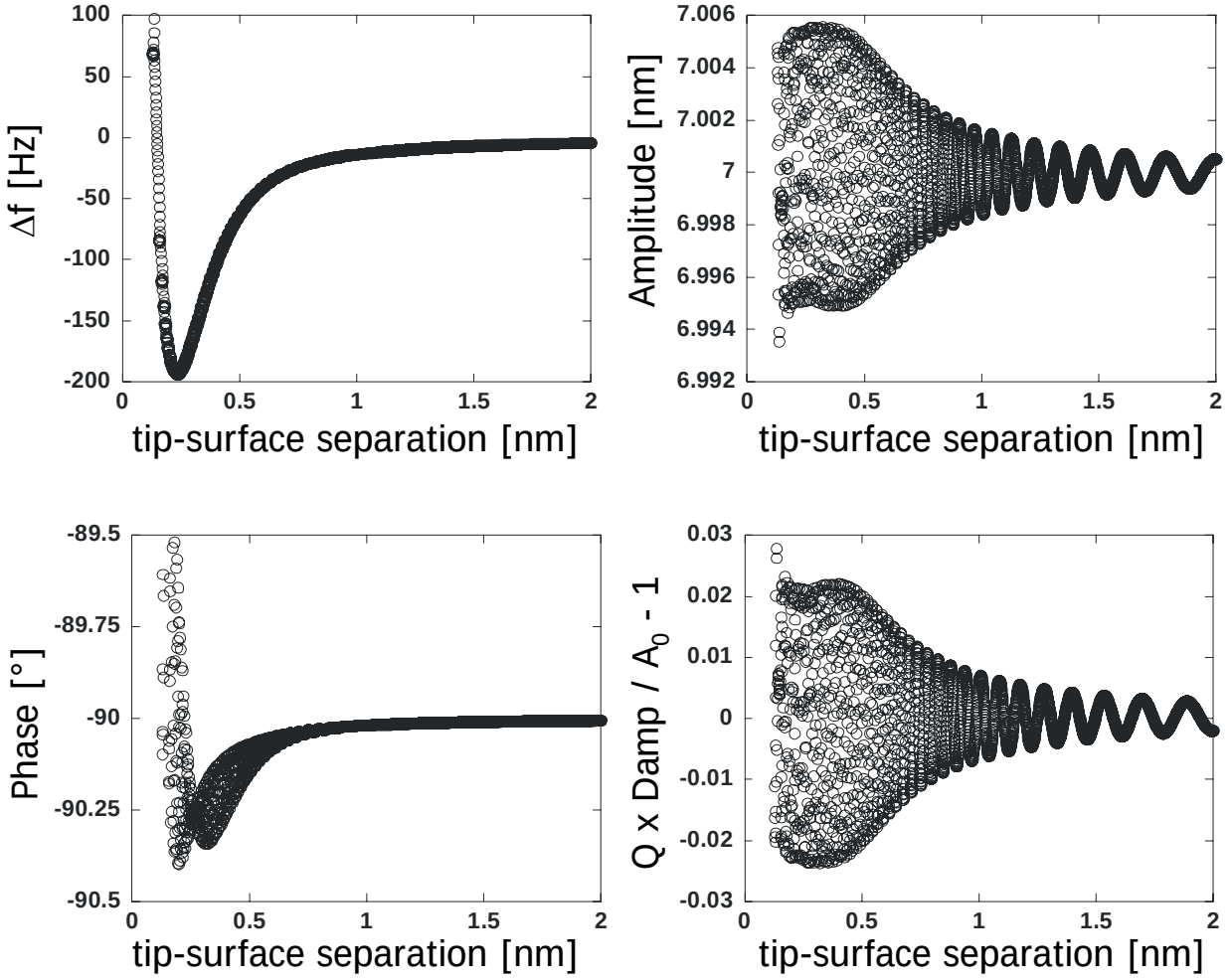

Validation of the virtual setup (2)

• Comparison with analytic expressions which do not take into account the finite response of the controllers, valid if $k_c A_0 >> |F_{int}|$:

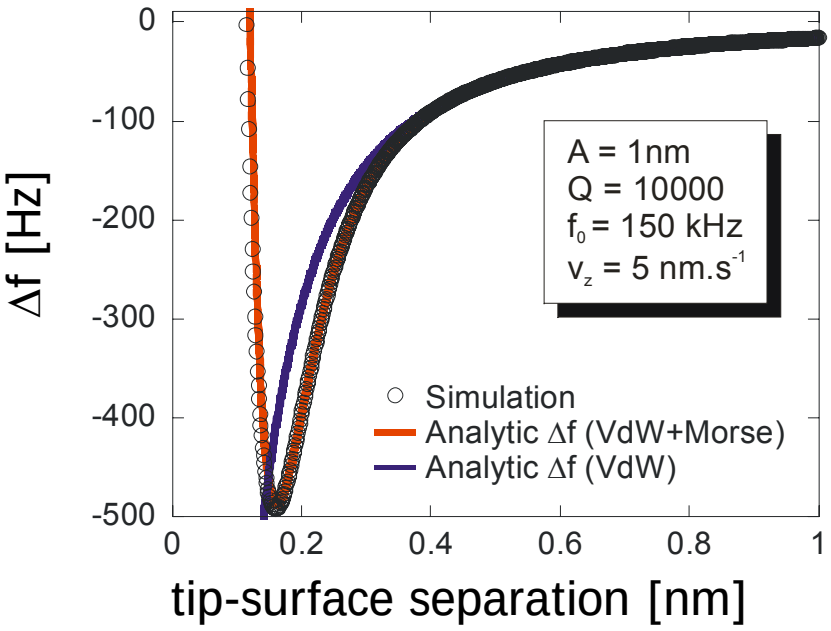

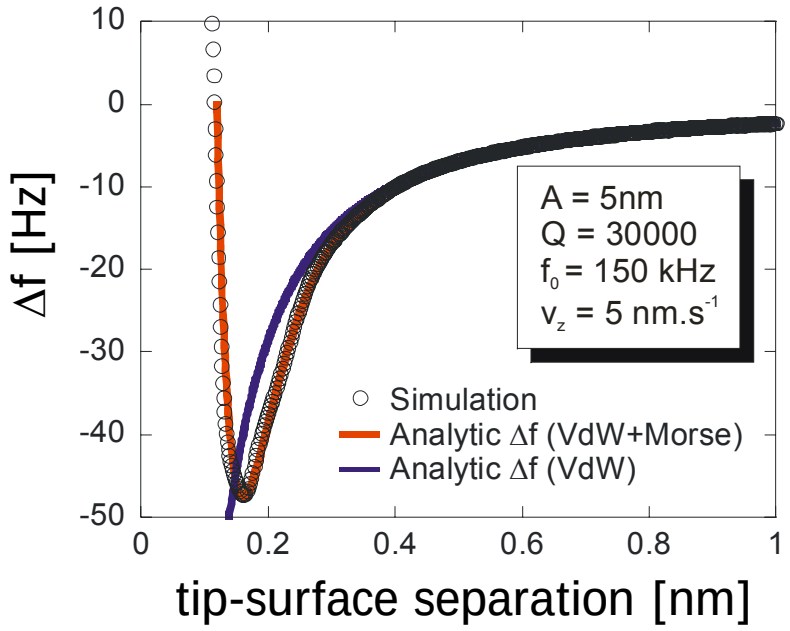

Dynamic properties of the PLL

- Step response (-10 Hz) analysis and fit with a decaying exponential :

Real PLL

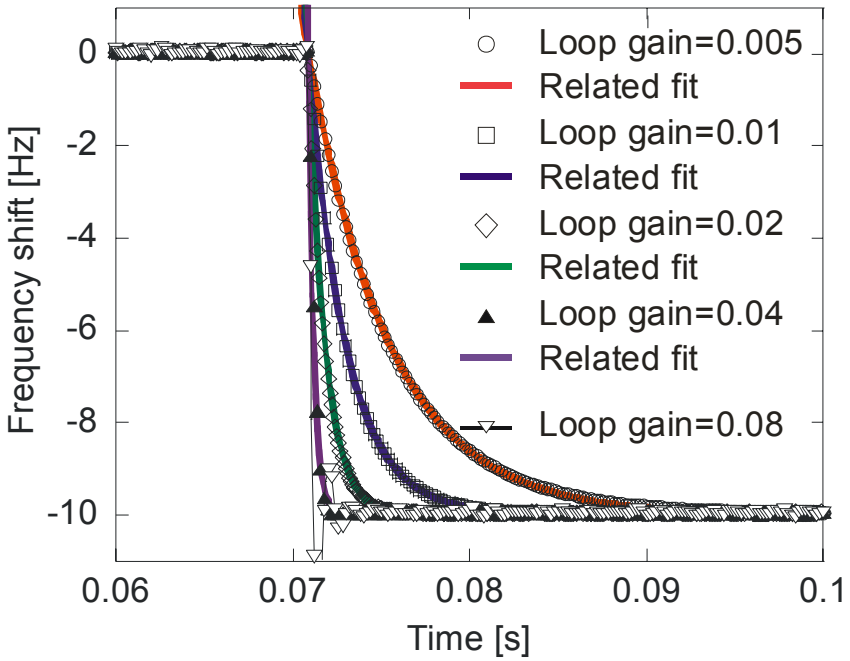

Virtual PLL

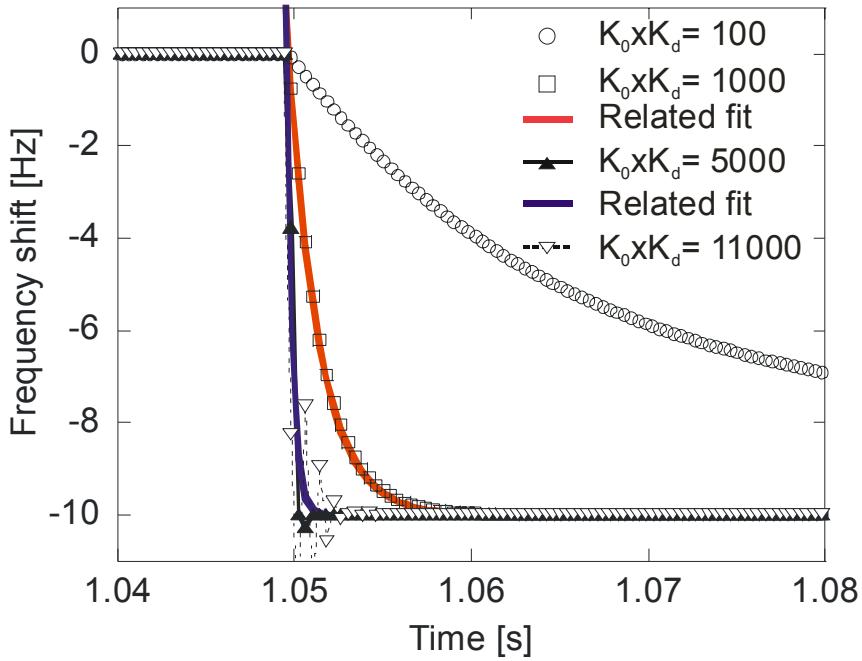

Dynamic properties of the PLL

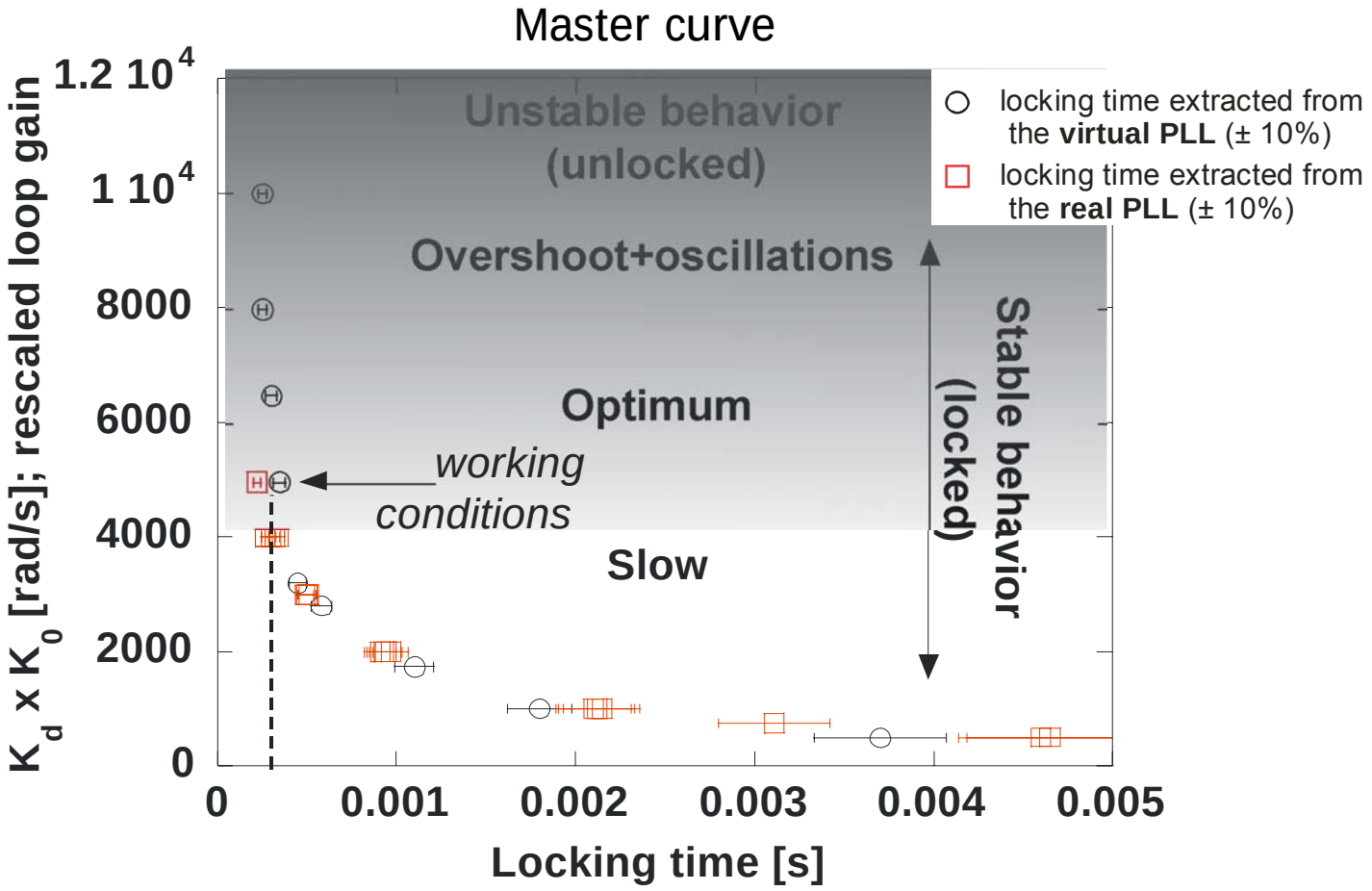

Optimum conditions t_{PLL} ~ 0.35 ms

The (key) role of the frequency tracker

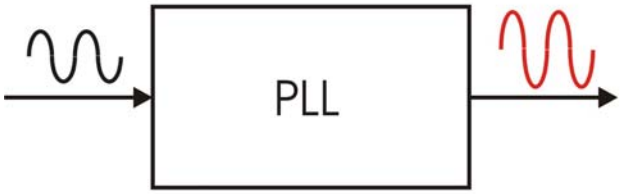

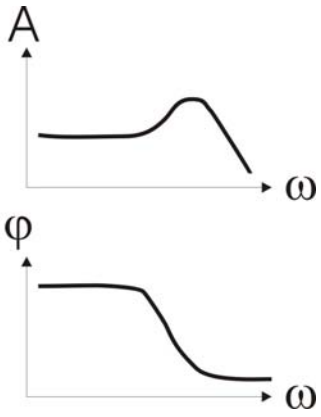

Upon approaching the surface, the frequency shifts :

Frequency tracker disengaged

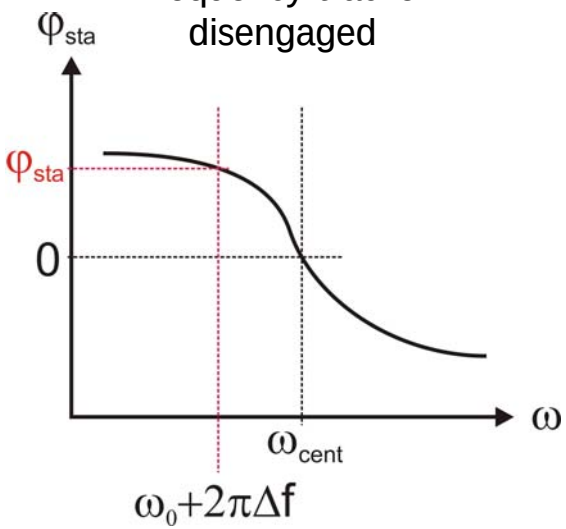

Frequency tracker engaged

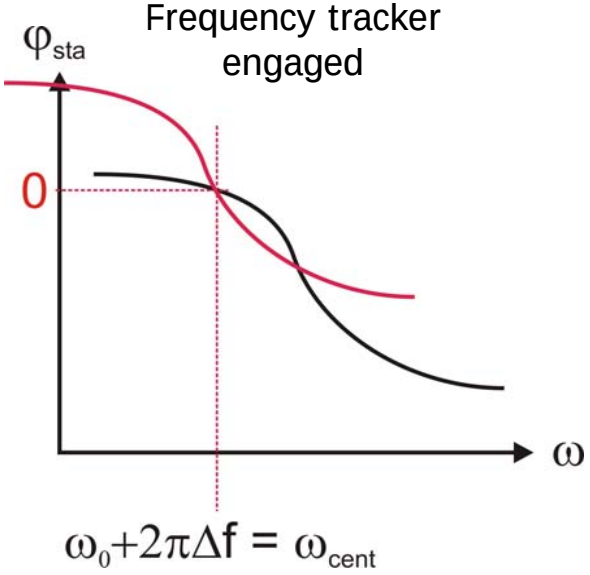

The (key) role of the frequency tracker

Frequency tracker disengaged

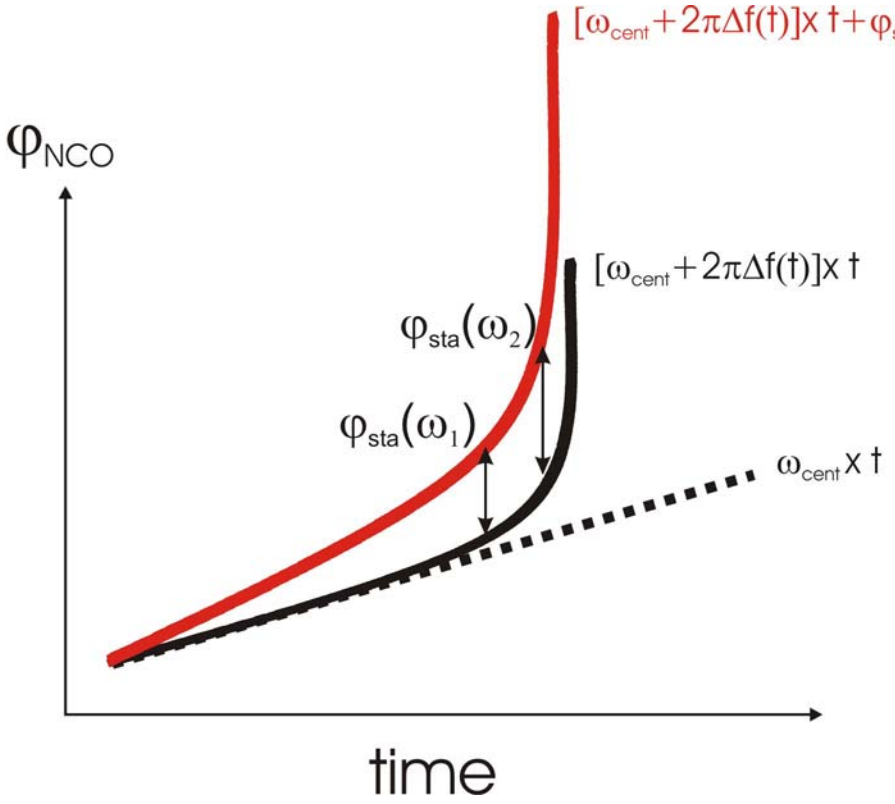

Frequency tracker engaged

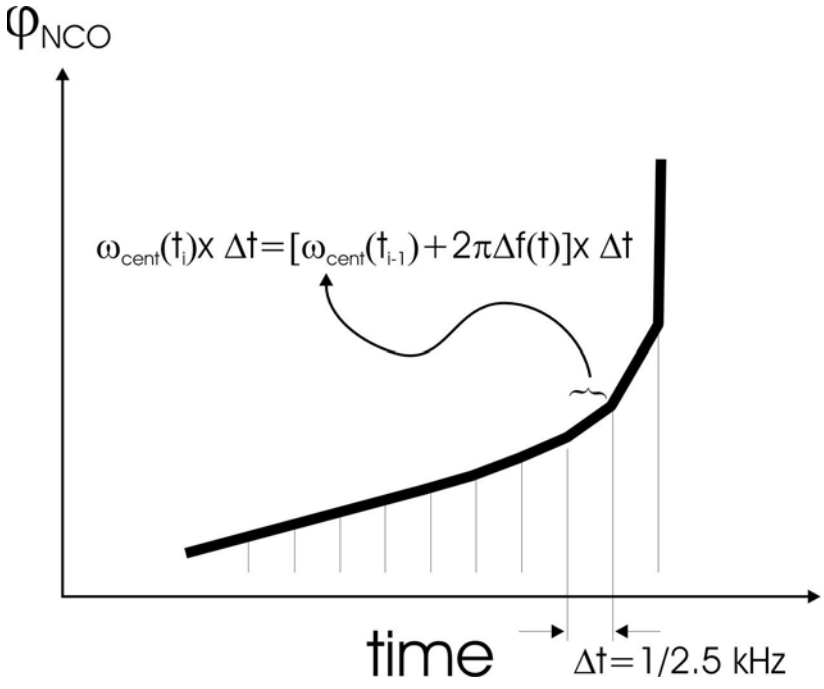

With the current design, the PLL locks **the time dependent phase** of the input signal **but can generate an additional static phase lag**

The (key) role of the frequency tracker

Frequency tracker disengaged

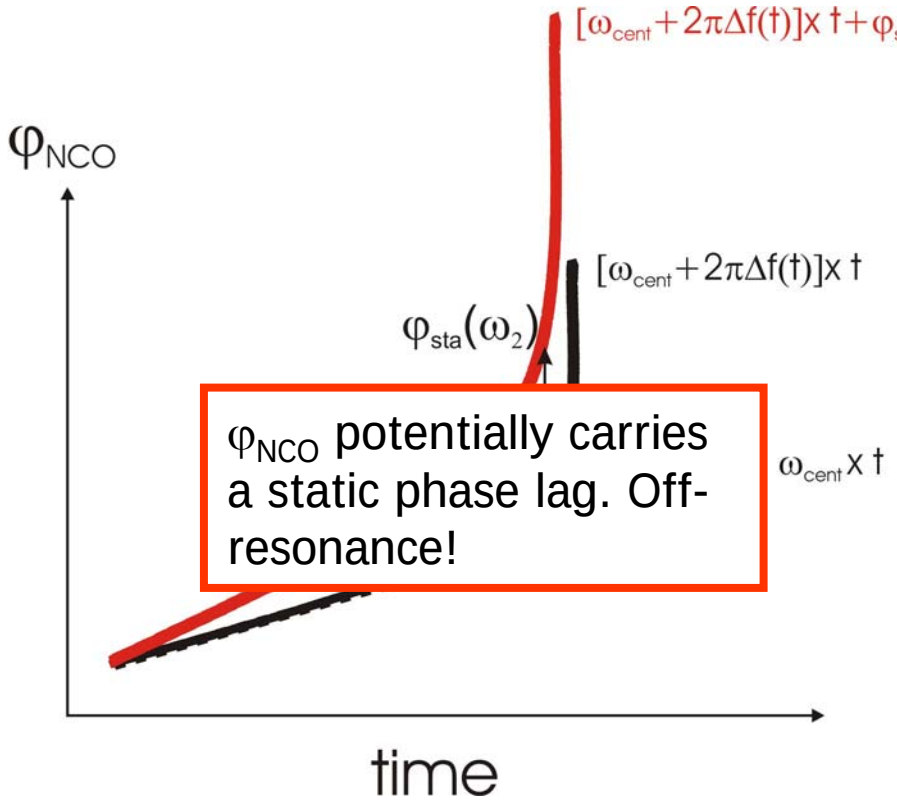

φ_{NCO} potentially carries a static phase lag. Off-resonance!

Frequency tracker engaged

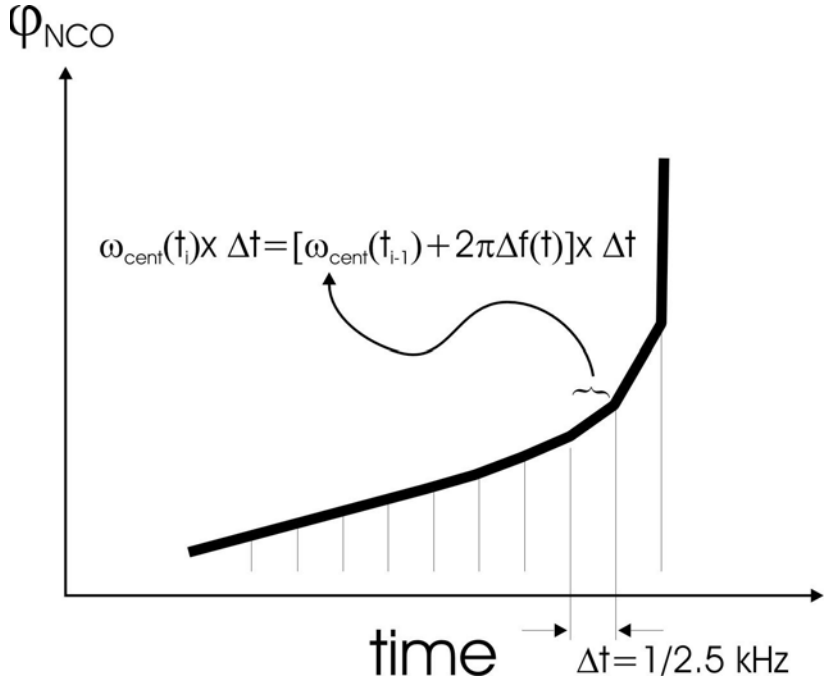

With the current design, the PLL locks **the time dependent phase** of the input signal **but can generate an additional static phase lag**

Experimental illustration

The PLL is fed with a 150 kHz sinusoidal waveform, the frequency of which is slowly detuned. The phase shift between input and output is monitored with a lock in amplifier.

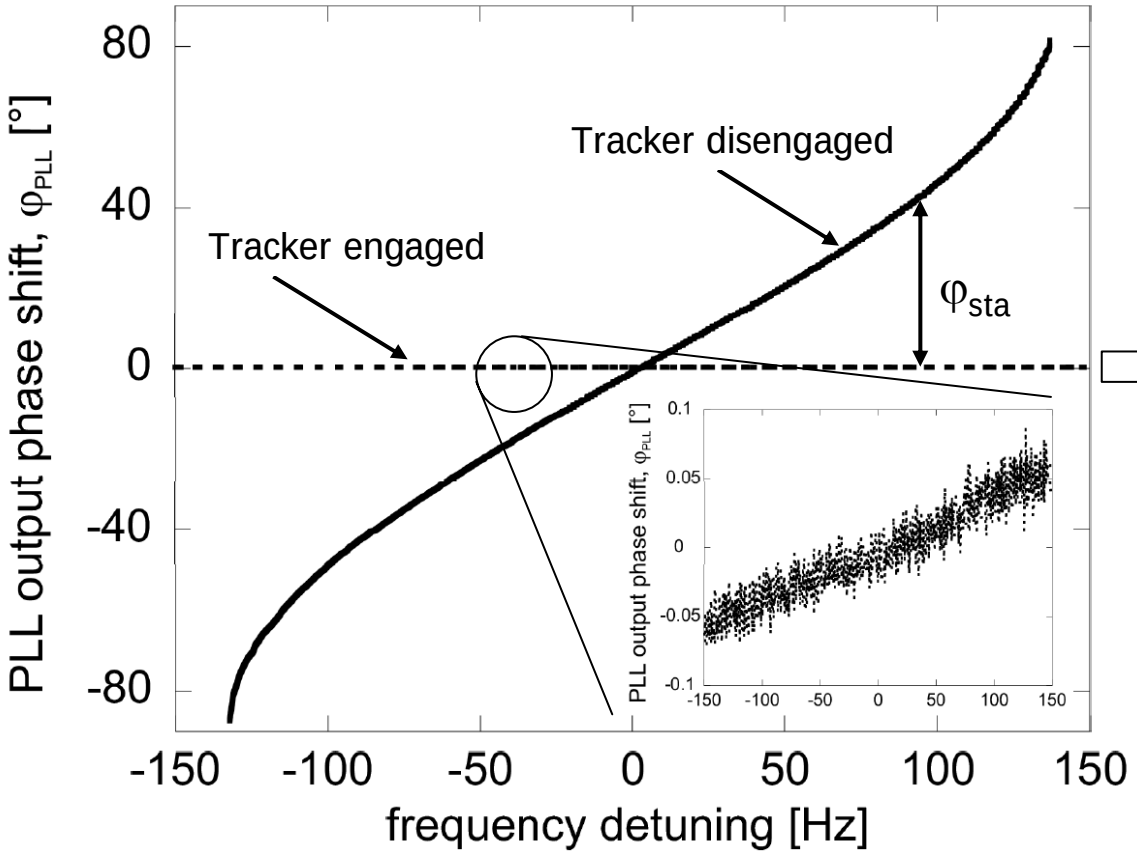

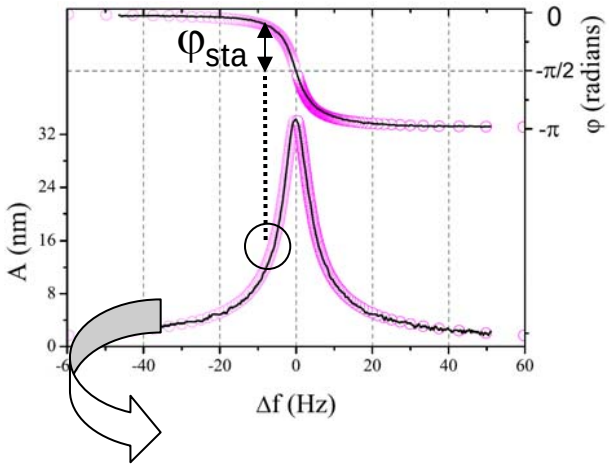

System driven off resonance
→ **amplitude drops down**
→ **apparent damping**

Dynamic properties of the APIC

• Step response (A_{RMS}x2) analysis and fit with a decaying exponential for the lone pairs of P,I gains leading to a **critically damped response**:

Real PLL

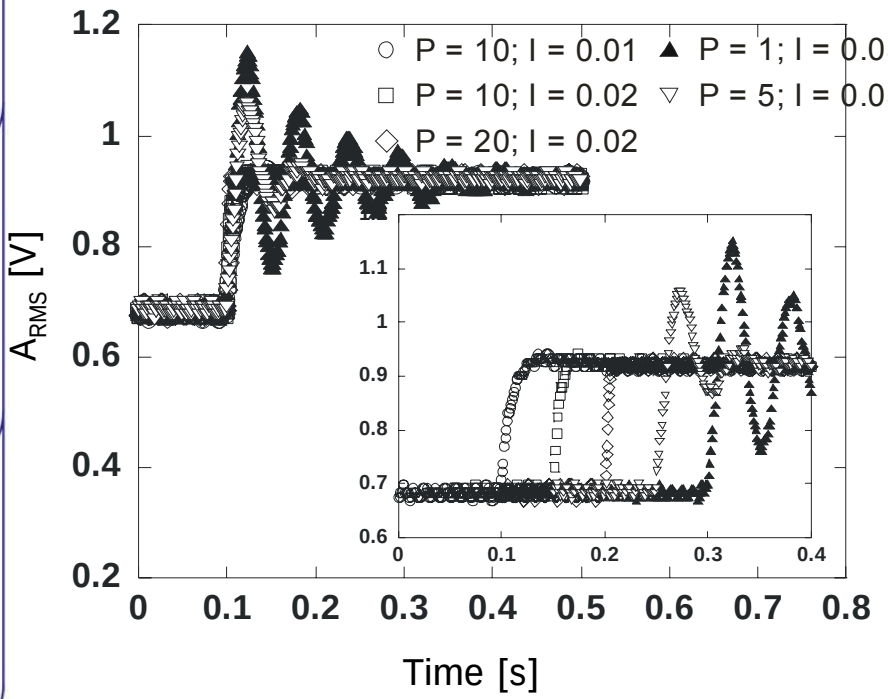

Virtual PLL

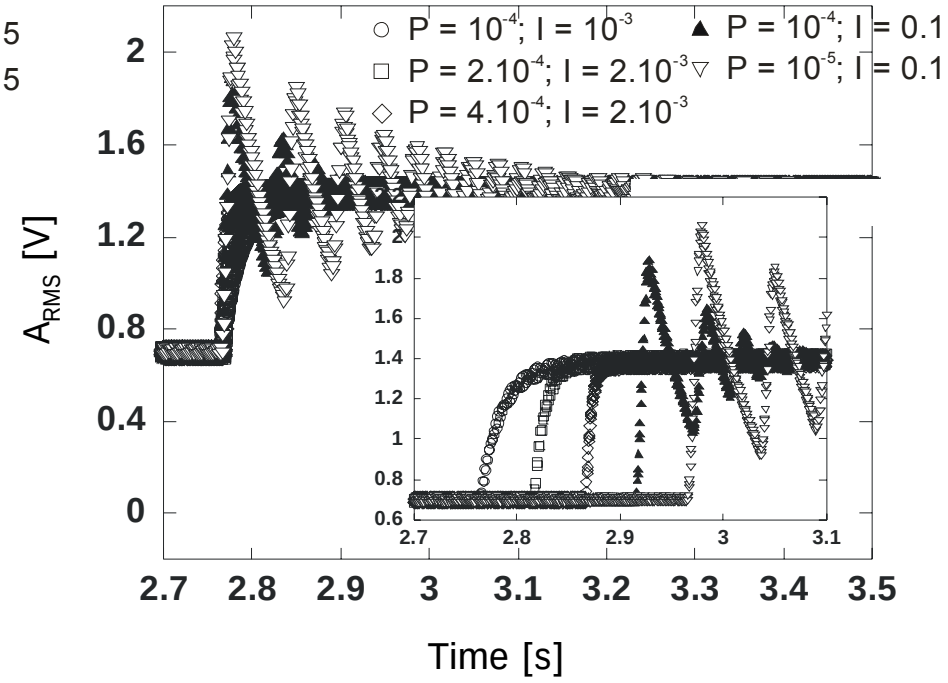

Dynamic properties of the APIC

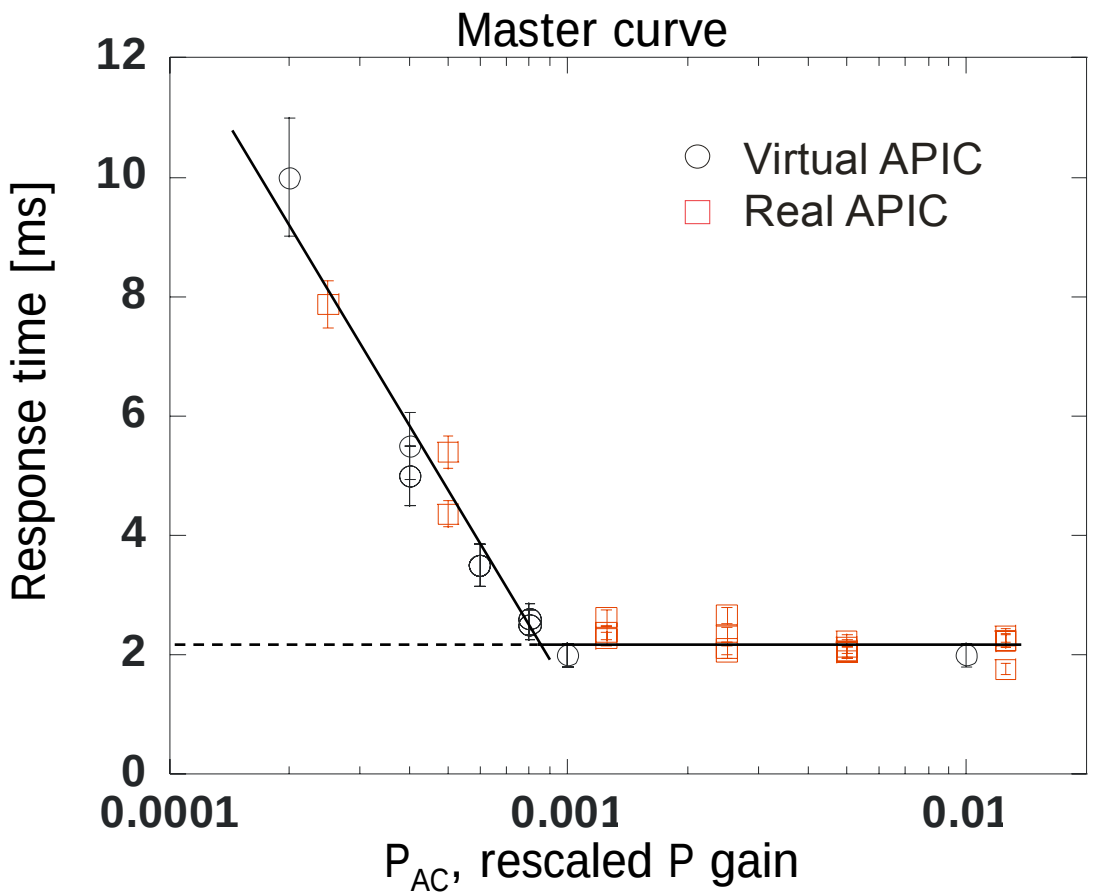

Optimum conditions t_{APIC} ~ 2.1 ms

Approach curves : apparent damping (1)

- Contribution of the PLL locking time: varying K_0 x K_d (frequency tracker engaged)

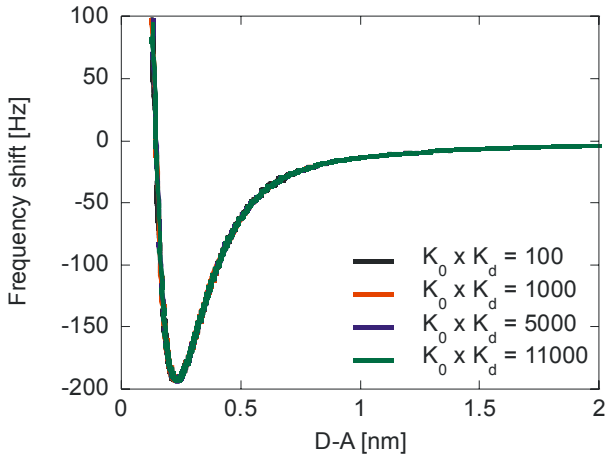

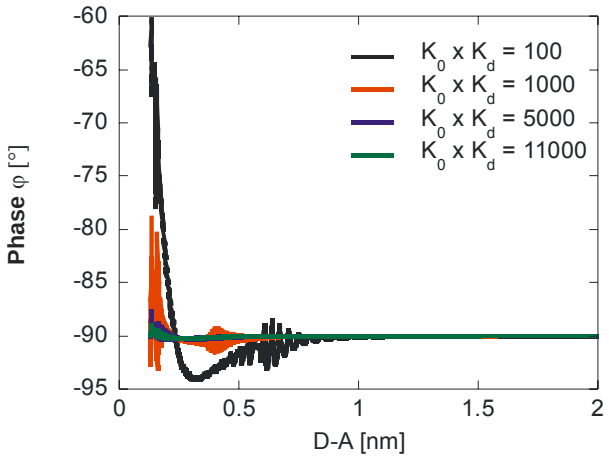

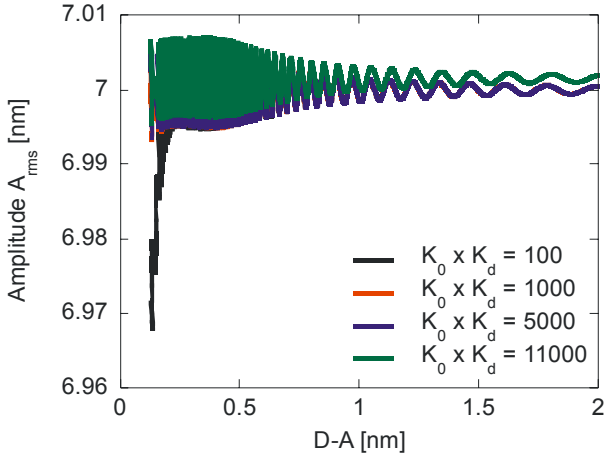

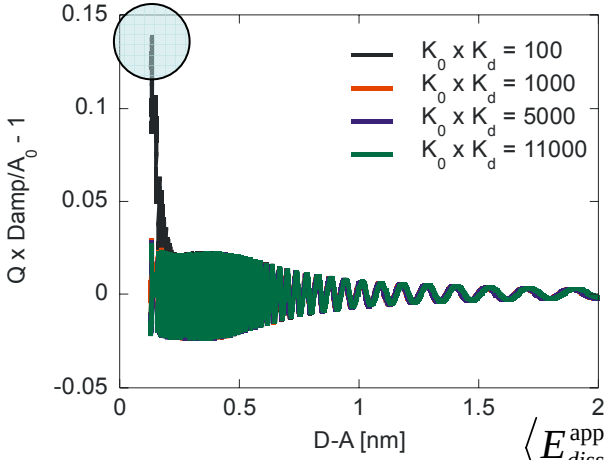

K_0K_d=100 ; t_{lock}>5 ms
K_0K_d=1000 ; t_{lock} ~ 2 ms
K_0K_d=5000 ; t_{lock} ~ 0.35 ms
K_0K_d=11000 ; t_{lock} < 0.2 ms (nervous)

Intrinsic damping :

$$\left\langle E_{diss}^{\text{intr}} \right\rangle_T = 2\,\text{eV/cycle}$$

Apparent damping :

$$\left\langle E_{diss}^{\text{app}} \right\rangle_T = 14\% \left\langle E_{diss}^{\text{intr}} \right\rangle_T \cong 0.28\,\text{eV/cycle}$$

Approach curves : apparent damping (2)

- Contribution of the frequency tracker

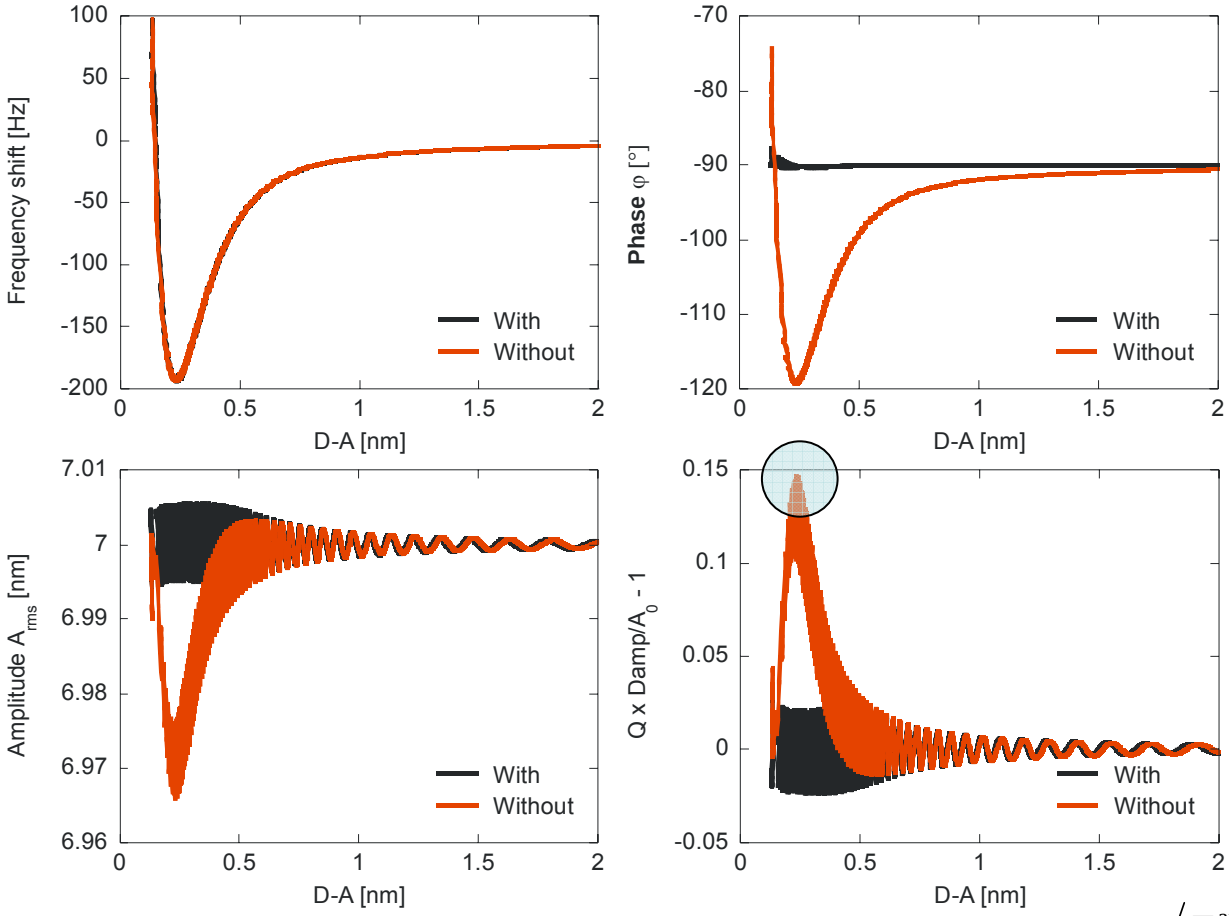

Apparent damping :

$$\left\langle E_{diss}^{app} \right\rangle_T = 14\% \left\langle E_{diss}^{intr} \right\rangle_T \cong 0.28\,\text{eV/cycle}$$

Summary

• **PLL dynamics** : **major role** in the occurrence of relevant **apparent damping** if the **locking time is about or larger than 1~ms**, that is only twice faster than the APIC optimum response time

• The **frequency tracker**, the aim of which is to update the PLL center frequency to make it matching the actual resonance frequency, plays also a **major role** in the occurrence of **apparent damping**. **It has to be engaged when performing approach curves**

• The **PLL optimal locking time is about 0.35 ms that is 6 times shorter than the shortest APIC response time** of the free cantilever. Therefore **the resonance condition is expected to be always properly maintained**. Consequently, when the PLL operates properly, **no amplitude changes due to a bad tracking of the resonance frequency are expected to occur**

• The APIC response time seems to be limited to ~2 ms due to the RMS-to-DC converter

Scan lines (Δf regulation) (1)

- Contribution of the PLL
  - Sinusoidally corrugated surface (λ = 6.6 Å)
  - 256 points per line
  - v_x=7 nm.s^{-1}, P_{AC}=10^{-3}, I_{AC}=10^{-4} s^{-1}
  - Frequency tracker engaged

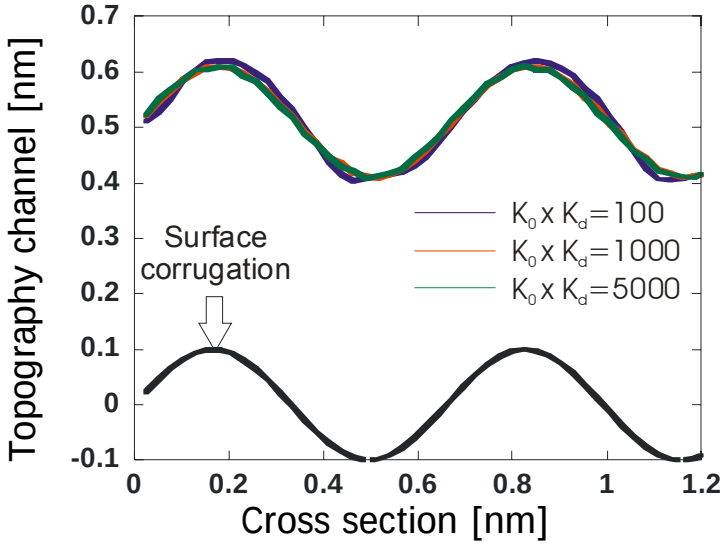

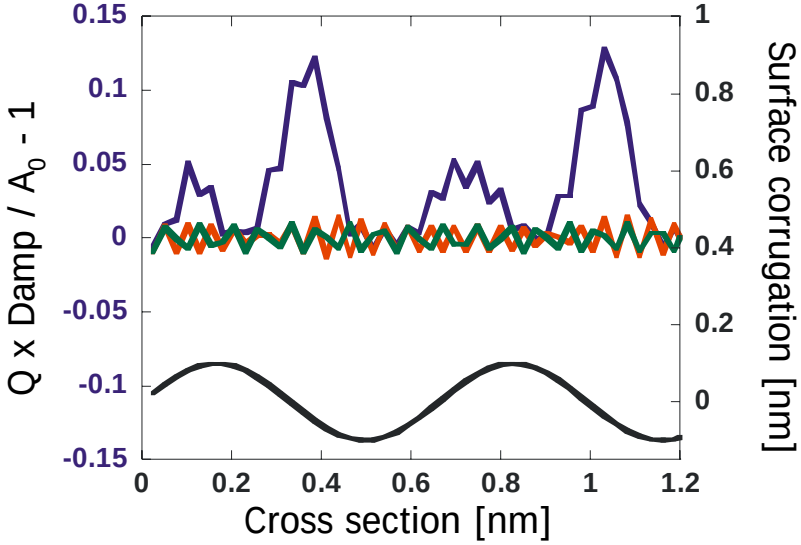

➡ Negligible effect on the topography
Negligible apparent damping except if PLL is slow

Scan lines (Δf regulation) (2)

- Contribution of the APIC
  - Surface with opposite steps (height : 3.3 Å)
  - 1024 points per line
  - v_x = 5 nm.s^{-1}, $K_0 x K_d$=5000 rad.s^{-1}
  - Frequency tracker engaged

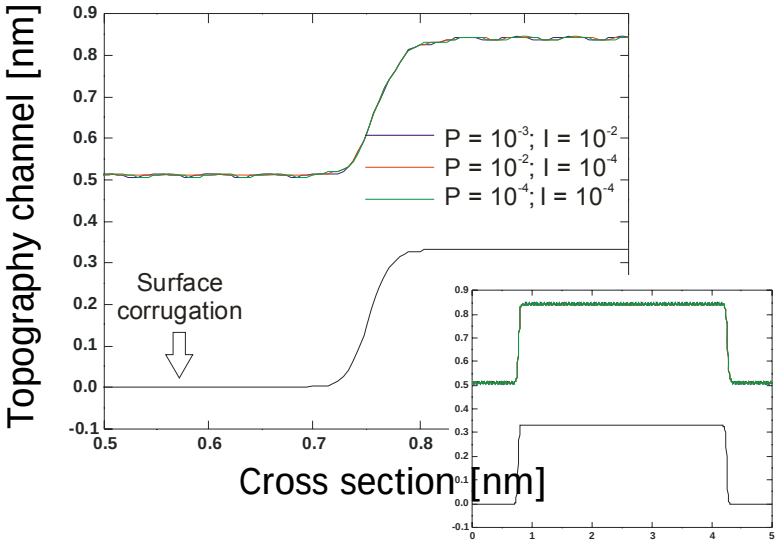

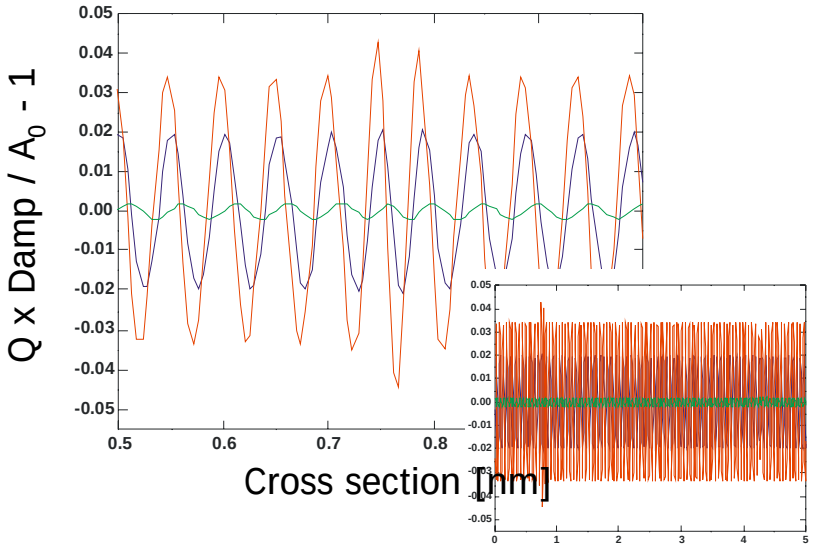

➡ Negligible effect on the topography
Weak apparent damping (not experimentally relevant) provided APIC is fast

Scan lines (Δf regulation) (3)

- Contribution of the scanning speed
  - Surface with opposite steps (height : 3.3 Å)
  - 256 points per line
  - $P_{AC}=10^{-3}$, $I_{AC}=10^{-4}$ s^{-1}, $K_0xK_d=5000$ $rad.s^{-1}$
  - Frequency tracker engaged

1 nm/s
2 nm/s
5 nm/s
10 nm/s
20 nm/s

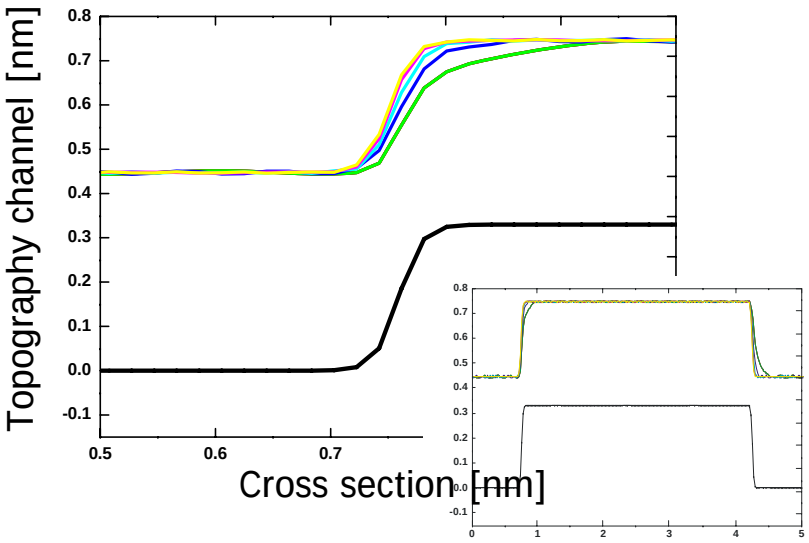

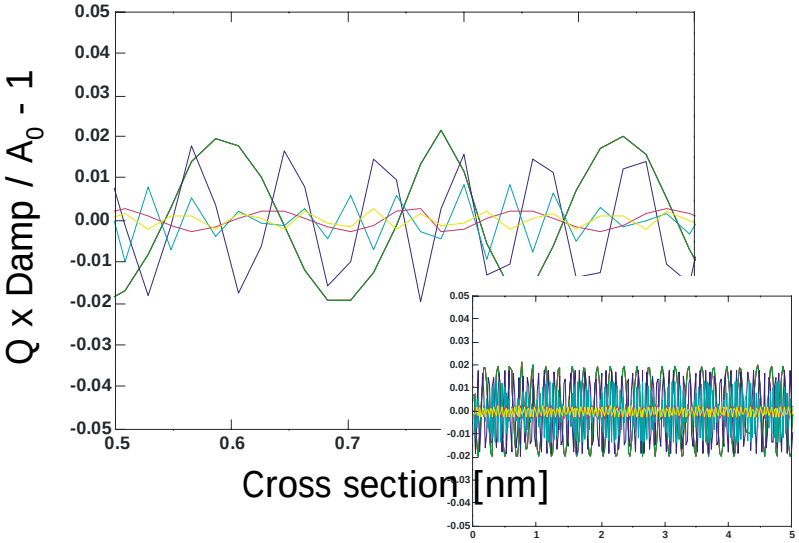

➡ { Distorted topography at high v_x
Weak apparent damping (not experimentally relevant)

Summary

• PLL dynamics : major role in the occurrence of relevant apparent damping if the locking time is about or larger than 1~ms, that is only twice faster than the APIC optimum response time

• The frequency tracker, the aim of which is to update the PLL center frequency to make it matching the
actual resonance frequency, plays also a major role in the occurrence of apparent damping. It has to be engaged when performing approach curves

• The PLL optimal locking time is about 0.35 ms that is 6 times shorter than the
shortest APIC response time of the free cantilever. Therefore the resonance condition is expected to be always properly maintained. Consequently, when the PLL operates properly, no amplitude changes due to a bad tracking of the resonance frequency are expected to occur

• The APIC response time seems to be limited to ~2 ms due to the RMS-to-DC converter

• **A weak contribution of the APIC to apparent dissipation is observed**. Although spatial shift and
apparent dissipation can conditionally be generated, the overall strength of the effect
remains weak and should hardly be measurable for UHV investigations at room temperature.

Is the apparent damping relevant?

Simplest assumption: what is the dissipated energy of the cantilever due to thermal fluctuations when oscillating close to the surface?

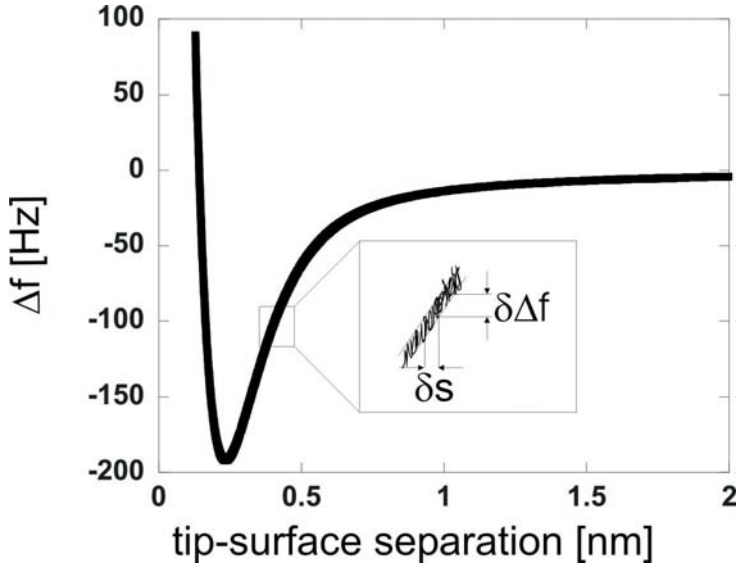

$k_BT \Rightarrow \delta A_0\ (\delta s) \Rightarrow \delta F_{int}\ (\delta \Delta f) \Rightarrow \delta A_{exc}$

To first order:

$$\frac{\delta A_{\rm exc}}{A_0} = \frac{\delta F_{\rm int}}{k_c A_0} \quad \Rightarrow \quad \delta E_d = \pi A_0 \delta F_{\rm int}$$

Δf is connected to F_{int} [1]:

$$\frac{\Delta f k_c A_0^{3/2}}{f_0} \simeq 0.43\sqrt{V_{\rm int}(r)F_{\rm int}(r)} \quad \Rightarrow \quad \frac{\delta f}{f_0} \simeq \frac{0.43}{2k_c A_0^{3/2}}\sqrt{\frac{V_{\rm int}(r)}{F_{\rm int}(r)}}\delta F_{\rm int}$$

The frequency noise is given by [2]:

$$\frac{\delta f}{f_0} = \sqrt{\frac{2k_BTB}{\pi^3 k_c A_0^2 f_0 Q}} \quad \Rightarrow \quad \boxed{\delta E_d \simeq 4.6\sqrt{\frac{2k_BTBk_c A_0^3 F_{\rm int}(r)}{\pi f_0 Q V_{\rm int}(r)}}}$$

[1]- H.-J. Ke *et al.*, **Noncontact Atomic Force Microscopy**, Eds Morita, Wiesendanger, Meyer, Springer Berlin, Germany 2002
[2]- F.J. Giessibl, ch2 in ref.[1]

Is the apparent damping relevant?

Parameters : A_0=7nm, f_0=150 kHz, k_c=40 Nm^{-1}, B=260 Hz
interaction parameters taken from [1] at s=5 Å

Q	E_0 (eV/cycle)	δE_d (eV/cycle)	$\delta E_d/E_0$	δE_d (eV/cycle)	$\delta E_d/E_0$
		VdW + short range		Pure VdW	
5000 ($T = 298°K$)	7.69	0.177	2.30%	0.141	1.84%
30000 ($T = 298°K$)	1.28	7.25×10^{-2}	5.65%	5.78×10^{-2}	4.50%
500000 ($T = 4°K$)	0.077	2.06×10^{-3}	2.67%	1.64×10^{-3}	2.13%

- Apparent dissipation due to PLL would be detected if it would occur (15%)
- Gauthier *et al.* put in evidence effects that are in the 5% range, not relevant in UHV at room temperature! With the conditions given in his work:

$\delta E_d/E_0 \sim$ 27%

Does not explain the shift but dissipation observed at steps is likely real dissipation

[1]- R. Pérez *et al.*, Phys. Rev. B **58**, 10835 (1998)

Summary and Outlooks

- ✓ Implementation of the real setup
- ✓ Reasonable description of the dynamic properties of the PLL (amplitude controller as well)
- ✓ Relevant apparent dissipation can conditionally be observed (PLL gains and frequency tracker)

- ❑ Investigation of the stability
- ❑ Contribution of noise
- ❑ Realistic force fields (SciFi)
- ❑ Atomistic description of damping
- ❑ Calculation of images

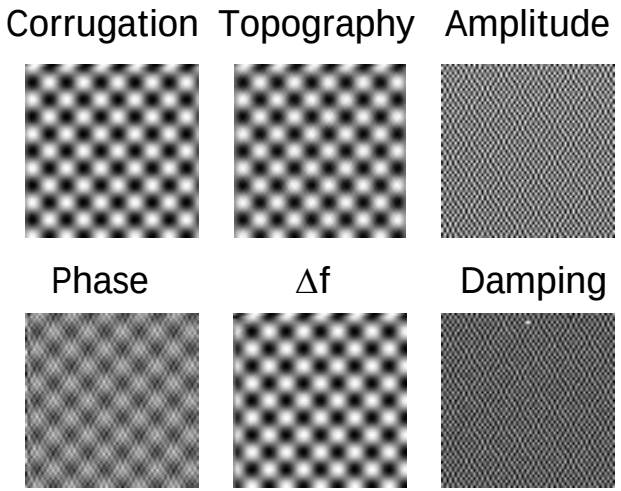

Questions / Discussions

Dynamic properties of the APIC

Behavior of the APIC in the closed loop:

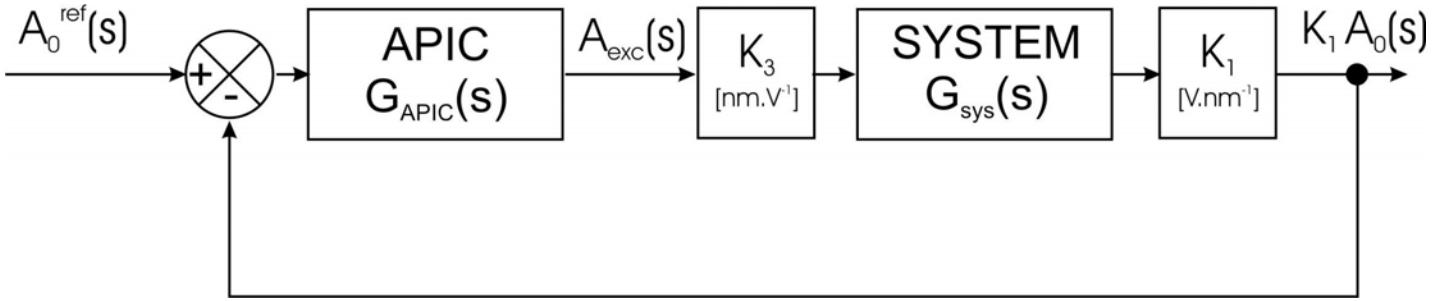

- Steady equation of the oscillator amplitude ($\varphi=-\pi/2$, $\omega=\omega_0$) :

$$G_{sys}(s) = \frac{K_1 A_0(s)}{A_{exc}(s)} = \frac{b}{s+a} \quad \begin{cases} b = \frac{K_1 K_3 \omega_0}{2} \\ a = \frac{\omega_0}{2Q} \end{cases}$$

$$\Rightarrow \quad G_{cl}(s) = \frac{K_1 A_0(s)}{A_0^{ref}(s)} = \frac{G_{APIC}(s) G_{sys}(s)}{1 + G_{APIC}(s) G_{sys}(s)}$$

- P, I controller :

$$G_{APIC}(s) = K_P + \frac{K_I}{s}$$

Dynamic properties of the APIC

The closed looped system is analogous to a second order system

$$\begin{cases} \text{Undercritically damped regime } \Rightarrow \zeta < 1 \Leftrightarrow c < \sqrt{bK_I} \\ \text{Critically damped regime } \Rightarrow \zeta = 1 \Leftrightarrow c = \sqrt{bK_I} \\ \text{Overcritically damped regime } \Rightarrow \zeta > 1 \Leftrightarrow c > \sqrt{bK_I} \end{cases} \qquad c = \frac{a + bK_P}{2}$$

$$K_I = \frac{\omega_0}{8}\left(\frac{1}{Q} + K_1 K_3 K_P\right)^2$$

⇩

time constant
of the system?

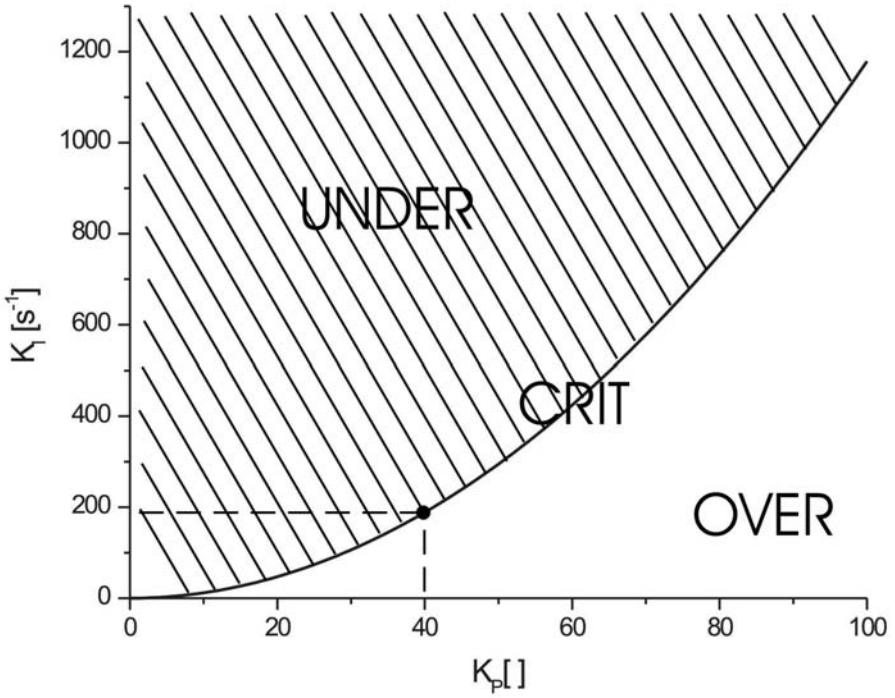

Dynamic properties of the APIC

Analysis of the system response to a step :

$$L^{-1} \quad G_s(s) = \frac{A_s}{s}$$

- Overcritically damped regime :

$$g_{cls}(t) = A_s \left\{ 1 + \frac{c-\xi-bK_P}{2\xi} e^{-(c+\xi)t} - \frac{c+\xi-bK_P}{2\xi} e^{-(c-\xi)t} \right\} \qquad \xi = \sqrt{c^2 - bK_I}$$

Short time scales

- Critically damped regime :

$$g_{cls}(t) = A_s \left\{ 1 - e^{-ct} + [bK_P - c]\, t e^{-ct} \right\}$$

- Undercritically damped regime :

$$g_{cls}(t) = A_s \left\{ 1 - e^{-ct} \times \left[\cos(\xi' t) + \frac{c-bK_P}{\xi'} \sin(\xi' t) \right] \right\} \qquad \xi' = \sqrt{bK_I - c^2}$$

Dynamic properties of the APIC

Summary :

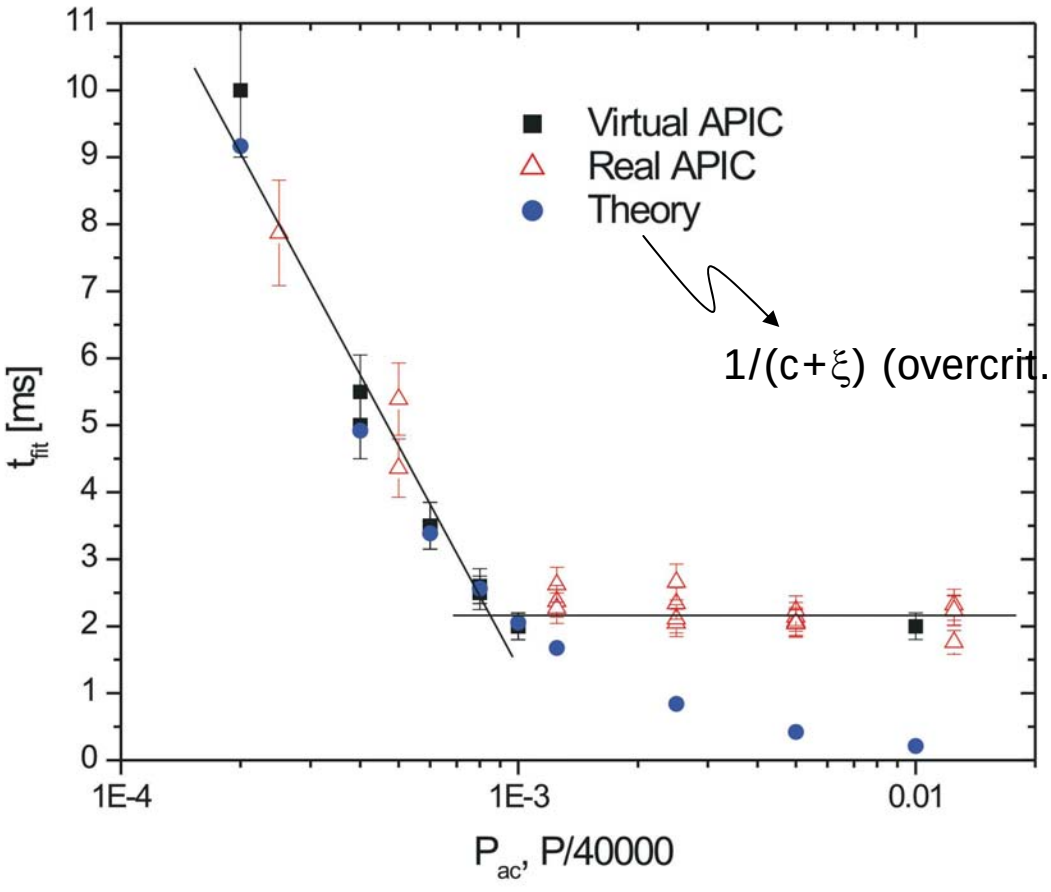

Remarks

- Time of calculation on a AMD 1700+, 512 Mb RAM
  - Approach curve: 15 nm vertical extension @ 2 $nm.s^{-1}$ ~ 45 min.
  - 1 scan line: 7 nm @ $5nm.s^{-1}$ ~ 20 min.

The digital filtering

Consists of $1/N_{ds}$ downsampling & LP-FIR filter:

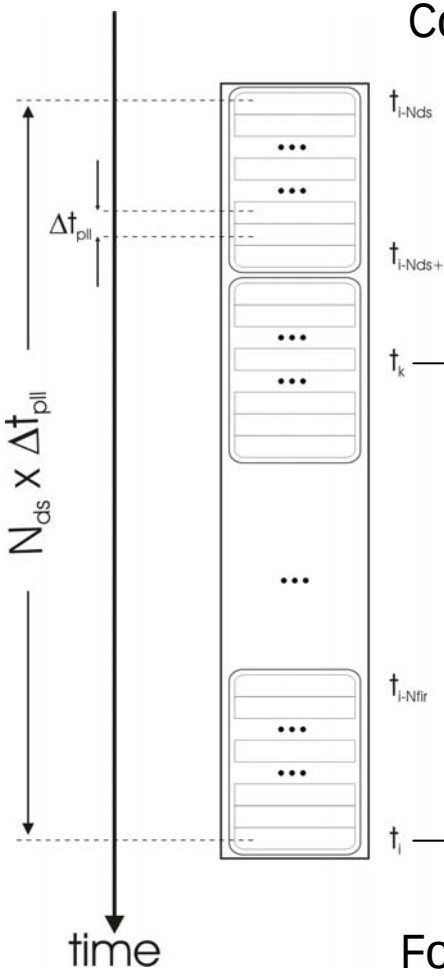

$$B(t_k) = \frac{\sum_{j=i-N_{ds}}^{k} K_d \times z_e(t_j)}{k-(i-N_{ds})+1} \quad \forall\ k \in [i - N_{ds}; i]$$

$$u_f(t_i) = \sum_{k=i-N_{fir}}^{i} c_k \times B(t_k)$$

For the 3 kHz low pass filter, N_{ds}=400 and N_{fir}=19

Stability analysis of the linear closed looped system

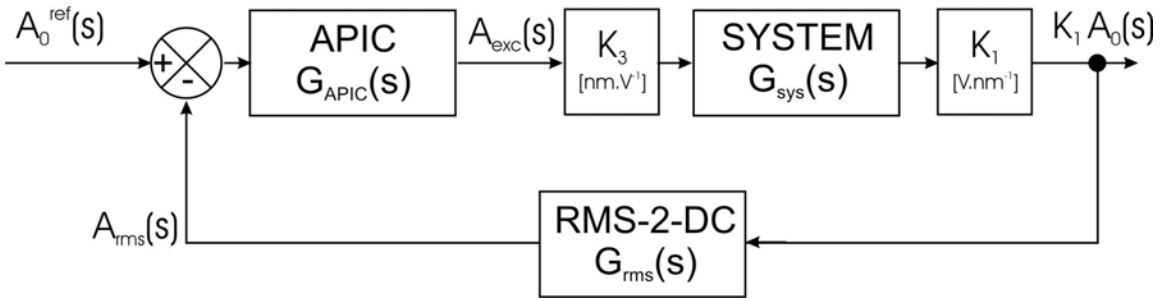

1st order steady equations

$$\begin{cases} \ddot{A}(t) = A(t)\left[\omega + \dot{\varphi}(t)\right]^2 - A(t)\omega_0^2 + K_3 A_{exc}(t)\omega_0^2 \cos(\varphi(t)) - \frac{\omega_0}{Q}\dot{A}(t) \\ \ddot{\varphi}(t) = -\frac{2\dot{A}(t)}{A(t)}\left[\omega + \dot{\varphi}(t)\right] - \frac{K_3 A_{exc}(t)\omega_0^2}{A(t)}\sin(\varphi(t)) - \frac{\omega_0}{Q}\left[\omega + \dot{\varphi}(t)\right] \\ K_3\dot{A}_{exc}(t) = -K_1K_3K_P dA(t) + K_3K_p dA_{rms}(t) + K_3K_I\left[A_0^{ref} - A_{rms}(t)\right] \\ \frac{\dot{A}_{rms}(t)}{K_1} = dA(t) - d\frac{A_{rms}(t)}{K_1} \end{cases}$$

$$\begin{pmatrix} \dot{\Lambda} \\ \dot{P} \\ \Lambda \\ P \\ K_3\dot{x} \\ \dot{r}/K_1 \end{pmatrix} = M \begin{pmatrix} \dot{\alpha} \\ \dot{p} \\ \alpha \\ p \\ K_3 x \\ r/K_1 \end{pmatrix} \quad \text{with} \quad M = \begin{pmatrix} -\frac{\omega_0}{Q} & 2\omega A^s & \omega^2 - \omega_0^2 & -\frac{A^s\omega_0^2}{Q}\sin(\varphi^s) & \omega_0^2\cos(\varphi^s) & 0 \\ -\frac{2\omega}{A^s} & -\frac{\omega_0}{Q} & -\frac{\omega_0\omega}{QA^s} & -\frac{\omega_0^2}{Q}\cos(\varphi^s) & -\frac{\omega_0^2}{A^s}\sin(\varphi^s) & 0 \\ 1 & 0 & 0 & 0 & 0 & 0 \\ 0 & 1 & 0 & 0 & 0 & 0 \\ 0 & 0 & -K_1K_3K_pd & 0 & 0 & K_1K_3(K_pd - K_i) \\ 0 & 0 & d & 0 & 0 & -d \end{pmatrix}$$

Stability analysis of the linear closed looped system

Resonance condition: $\varphi=-\pi/2$, $\omega=\omega_0$

Rooth-Hurwitz stability analysis $\Rightarrow$ 5 determinants : Δ_1, Δ_2, Δ_3, Δ_4, Δ_5.
Must be **positive** for the system to be **stable**

Δ_1 and Δ_2 are unconditionally positive